ESAIM: M2AN 53 (2019) 749–774
https://doi.org/10.1051/m2an/2018074

ESAIM: Mathematical Modelling and Numerical Analysis
www.esaim-m2an.org

THE NONCONFORMING VIRTUAL ELEMENT METHOD FOR EIGENVALUE PROBLEMS

Francesca Gardini[1,*], Gianmarco Manzini[2] and Giuseppe Vacca[3]

Abstract. We analyse the nonconforming Virtual Element Method (VEM) for the approximation of elliptic eigenvalue problems. The nonconforming VEM allows to treat in the same formulation the two- and three-dimensional case. We present two possible formulations of the discrete problem, derived respectively by the nonstabilized and stabilized approximation of the L^2-inner product, and we study the convergence properties of the corresponding discrete eigenvalue problem. The proposed schemes provide a correct approximation of the spectrum, in particular we prove optimal-order error estimates for the eigenfunctions and the usual double order of convergence of the eigenvalues. Finally we show a large set of numerical tests supporting the theoretical results, including a comparison with the conforming Virtual Element choice.

Mathematics Subject Classification. 65N30, 65N25.

Received February 8, 2018. Accepted November 29, 2018.

1. Introduction

The Virtual Element Method (in short, VEM) was introduced in [9] as a generalization of the finite element method to arbitrary polygonal and polyhedral meshes and as a variational reformulation of the Mimetic Finite Difference (MFD) method [10, 24]. The main idea behind VEM is that the approximation spaces consist of the usual polynomials and additional nonpolynomial functions that locally solve suitable differential problems. Consequently, the virtual functions are not explicitly known pointwisely (hence the name virtual), but only a limited set of information about them are at disposal. Nevertheless, the available information is sufficient to construct the discrete operators and the right-hand side. Indeed, the VEM does not require the evaluation of test and trial functions at the integration points, but uses suitable projections onto the space of piecewise polynomials that are exactly computable from the degrees of freedom. Therefore, the approximated discrete bilinear forms require only integration of polynomials on each polytopal element in order to be computed, without the need to integrate complex non-polynomial functions on the elements and without any loss of accuracy. Moreover the VEM can be easily applied to three dimensional problems and can handle non-convex (even non simply connected) elements [3, 15]. VEMs have been developed successfully for a large range of mathematical and

Keywords and phrases. Nonconforming virtual element, eigenvalue problem, polygonal meshes.

[1] Dipartimento di Matematica *F. Casorati*, Università di Pavia, Via Ferrata, 5 – 27100 Pavia, Italy.
[2] Group T-5, Theoretical Division, Los Alamos National Laboratory, Los Alamos, NM 87545, USA.
[3] Dipartimento di Matematica e Applicazioni, Università degli Studi di Milano Bicocca, Via R. Cozzi, 55 – 20125 Milano, Italy.
*Corresponding author: francesca.gardini@unipv.it

engineering problems [6, 11, 17, 19, 30, 33, 51–53]. Finally, high-order and higher-order continuity schemes have been presented in [4, 18, 25, 32], respectively.

The present paper focuses on the nonconforming VEM for the approximation of the second-order elliptic eigenvalue problem. The nonconforming VEM introduced in [7] shows a comparable accuracy with respect to the "standard" conforming VEM, as shown by the error plots *versus* the mesh size and the number of degrees of freedom reported in the final section on numerical experiments. Nonetheless, it offers several undisputed advantages with respect to the conforming VEM formulation and the classical nonconfoming finite element method. Indeed, it covers "in one shot", *i.e.*, using the same formulation, the two- and three-dimensional case; hence, no recursive construction from the low dimensional faces is needed. This feature makes the nonconforming VEM particularly appealing for applications that are inherently multidimensional as the Schrödinger equation. This will be the topic of future works. Moreover, the formulation of the nonconforming method works on polygonal and polyhedral elements with very general shapes. A unique analysis is possible for all the cases mentioned above.

We recall that for the nonconforming methods, the approximating space is not a subspace of the solution space. In particular, for second-order elliptic problems we do not require the H^1-regularity of the global discrete space as for the conforming schemes, but we just impose that the moments, up to a certain order, of the jumps of the discrete space functions across all mesh interfaces are zero.

The nonconforming VEM has been applied successfully to the general second-order elliptic problem [31], the Stokes equation [29], the biharmonic problem [5], and the nonconforming approach has been recently extended to the h- and p-version of the harmonic VEM [46]. As first observed in [7] and recently investigated in [38], the nonconforming VEM coincides with the high-order MFD method proposed in [45].

In the present paper, we study the nonconforming VEM for the approximation of the Laplace eigenvalue problem. Using the nonconforming virtual space introduced in [7], we introduce two approximated bilinear forms, one stands for the discrete grad-grad form and the other one stands for the discrete version of the L^2-inner product. In particular, for the L^2-inner product, we consider both a nonstabilized form and a stabilized one, and we study the convergence properties of the corresponding discrete formulations. The convergence analysis is carried out in the framework of Babuška-Osborne theory for the spectral approximation for compact operators [8]. The uniform convergence of the discrete solution operators to the continuous one follows from the *a priori* error estimates for the source problem [7]. We show that the nonconforming VEM provides optimal convergence rates both in the approximations of the eigenfunctions and eigenvalues. These results hold under minimal regularity assumption, *i.e.*, for eigenfunctions that are in H^{1+r} with $r > \frac{1}{2}$, thus, without requiring a convex-shaped domain. To this end, we generalize the *a priori* estimates of [7], which were proved assuming H^2-regularity.

We remark that the conforming VEM formulation has been proposed for the approximation of the Steklov eigenvalue problem [47, 48], the Laplace eigenvalue problem [42], the acoustic vibration problem [12], and the vibration problem of Kirchhoff plates [49], whereas [27] deals with the Mimetic Finite Difference approximation of the eigenvalue problem in mixed form. In the context of Hybrid High-Order (HHO) methods [37, 40], the spectral approximation analysis of elliptic operators has been recently presented in [26]. As shown in [35] the HHO method and the nonconforming VEM are closely related. For both methods the analysis is carried out in the framework of the abstract theory for the spectral approximation for compact operators. However, the different mathematical structure of the two numerical formulations implies a different approach in the way these theoretical tools are used in the analysis. Indeed, the HHO method is based on a "*two-fields*" formulation, which uses distinct polynomial approximations inside the mesh cells and on the mesh faces. For this reason the definition of the HHO discrete solution operator requires the elimination of the face unknowns, which is not an issue in our case.

The outline of the paper is as follows. In Section 2 we formulate the model Laplace eigenvalue problem. In Section 3 we introduce the broken Sobolev spaces (with respect to the polygonal decompositions) and we define the conformity error. Moreover we recall the definition of the nonconforming Virtual Element Spaces and their degrees of freedom. In Section 4 we construct the approximated bilinear forms and we state the nonconforming

virtual problem. In Section 5 we recall some fundamental results for the spectral approximation of compact operators. In Section 6 we show the optimal rate of convergence of the method by proving the *a priori* error estimates for the eigenvalues and eigenfunctions. Section 7 presents several numerical tests. Finally, in Section 8 we offer our final remarks and conclusions.

2. The continuous eigenvalue problem

In this section we describe the continuous eigenvalue problem and its associated source problem. Throughout the paper, we use the notation of Sobolev spaces, norms and seminorms detailed in [1]. Hence, for an open bounded domain ω of $\mathbb{R}^d$, norm and seminorm in $H^s(\omega)$ are denoted by $\|\cdot\|_{s,\omega}$, and $|\cdot|_{s,\omega}$, while $(\cdot,\cdot)_\omega$ and $\|\cdot\|_{0,\omega}$ denote L^2-inner product and L^2-norm, respectively. The subscript ω may be omitted when ω is the whole computational domain.

Let $\Omega \subset \mathbb{R}^d$ for $d = 2, 3$ be an open polytopal domain with Lipschitz boundary Γ, we are interested in the following problem: find eigenvalue λ and eigenfunction u with $u \neq 0$ such that

$$\begin{cases} -\Delta u = \lambda\, u & \text{in } \Omega \\ u = 0 & \text{on } \Gamma. \end{cases} \tag{2.1}$$

The variational formulation of problem (2.1) reads as follows:

$$\begin{cases} \text{find } (\lambda,\, u) \in \mathbb{R} \times V & \text{with } \|u\|_0 = 1 \text{ such that} \\ a(u,v) = \lambda\, b(u,v) & \text{for all } v \in V \end{cases} \tag{2.2}$$

where $V = H_0^1(\Omega)$, the bilinear form $a : V \times V \to \mathbb{R}$ is given by

$$a(u,v) = \int_\Omega \nabla u \cdot \nabla v \,\mathrm{d}\Omega \qquad \text{for all } u,\, v \in V, \tag{2.3}$$

and the bilinear form $b : V \times V \to \mathbb{R}$ is the L^2-inner product on Ω, *i.e.*,

$$b(u,v) = (u,v) \qquad \text{for all } u,\, v \in V. \tag{2.4}$$

The eigenvalues of problem (2.2) form a positive increasing divergent sequence and the corresponding eigenfunctions constitute an orthonormal basis of V with respect both to the L^2-inner product and the scalar product associated with the bilinear form $a(\cdot,\cdot)$. Moreover, each eigenspace has finite dimension [8,20].

In the spectral convergence analysis, we will need the approximation results of the source problem associated with (2.2), which we state as follows:

$$\begin{cases} \text{find } u^s \in V & \text{such that} \\ a(u^s, v) = b(f, v) & \text{for all } v \in V \end{cases} \tag{2.5}$$

where we assume the forcing term f (at least) in $L^2(\Omega)$. Due to regularity results [2,43], there exists a constant $r > 1/2$ that depends only on Ω such that the solution u^s belongs to the space $H^{1+r}(\Omega)$. In particular, if Ω is a convex polytopal domain, then $r \geq 1$. Instead, $r \geq \pi/\omega - \varepsilon$ for any $\varepsilon > 0$ if Ω is a two-dimensional non-convex polygonal domain with maximum interior angle $\omega < 2\pi$. A similar result holds for non-convex polyhedra, ω being the maximum reentrant wedge angle. Eventually, there exists a positive constant C such that

$$|u^s|_{1+r} \leq C \|f\|_0. \tag{2.6}$$

We will consider the virtual element discretization of source problem (2.5) in the form

$$\begin{cases} \text{find } u_h^s \in V_k^h & \text{such that} \\ a_h(u_h^s, v_h) = b_h(f, v_h) & \text{for all } v_h \in V_k^h \end{cases}$$

where V_k^h is the nonconforming virtual element space, a_h and b_h suitable virtual element approximation of the continuous bilinear form a and b. Similarly, we will seek for the virtual element discretization of the continuous eigenvalue problem (2.2) in the form:

$$\begin{cases} \text{find } (\lambda_h,\, u_h) \in \mathbb{R} \times V_k^h & \text{with } \|u_h\|_0 = 1 \text{ such that} \\ a_h(u_h, v_h) = \lambda_h\, b_h(u_h, v_h) & \text{for all } v_h \in V_k^h. \end{cases}$$

The definition of V_k^h and possible constructions of a_h and b_h in the nonconforming setting are the topic of the next section.

3. The nonconforming virtual element method

In the present section we describe the regularity assumptions of the mesh decompositions of the domain and we introduce the nonconforming functional spaces. Then we define the nonconforming virtual element space [7, 31] and related approximation properties that we need for the proper formulation of the virtual element method.

3.1. Mesh definition and regularity assumptions

Let $\mathcal{T} = \{\Omega_h\}_h$ be a family of decompositions of Ω into nonoverlapping polytopal elements P with nonintersecting boundary ∂P, d-dimensional measure $|P|$, and diameter h_P The subindex h that labels each mesh Ω_h is the maximum of the diameters h_P of the elements of that mesh. The boundary of P is formed by straight edges when $d = 2$ and flat faces when $d = 3$. We may refer to the geometric objects forming the elemental boundary ∂P by the term *side* instead of *edge/face* (for the two- and three-dimensional case respectively) and adopt a unified notation by using the symbol σ regardless of the number of spatial dimensions. Accordingly, h_σ, and $|\sigma|$ denote the diameter and measure of side σ.

We denote the unit normal vector to the elemental boundary ∂P by $\mathbf{n}_P$, and the unit normal vector to side σ by $\mathbf{n}_\sigma$. Each vector $\mathbf{n}_P$ points out of P and the orientation of $\mathbf{n}_\sigma$ is fixed *once and for all* in every mesh Ω_h. Finally, $\mathcal{E}_h$, $\mathcal{F}_h$, and $\mathcal{S}_h$ denote the set of edges, faces, and sides of the skeleton of Ω_h. We may distinguish between *internal* and *boundary* sides by using the superscript 0 and ∂. Therefore, $\mathcal{S}_h^0$ is the set of the internal sides, $\mathcal{S}_h^\partial$ the set of the boundary sides.

Now, we state the mesh regularity assumptions that are required for the convergence analysis. We suppose that for all h, each element P in Ω_h fulfils the following assumptions [9, 15]:

(A0³) Mesh regularity assumptions three-dimensional case

- P is star-shaped with respect to a ball with radius $\geq \varrho h_P$;
- every face $f \in P$ is star-shaped with respect to a disk with radius $\geq \varrho h_f$;
- for every edge $e \in \partial f$ of every face $f \in \partial P$ it holds that $h_e \geq \varrho h_f \geq \varrho^2 h_P$.

(A0²) Mesh regularity assumptions two-dimensional case

- P is star-shaped with respect to a disk with radius $\geq \varrho h_P$;
- for every edge $e \in \partial P$ it holds that $h_e \geq \varrho h_P$,

where ϱ is a uniform positive constant called mesh regularity constant. In the following we may refer to the two- and three-dimensional assumptions using the same label **(A0)**.

Remark 3.1. The star-shapedness property implies that elements and faces are *simply connected* subsets of $\mathbb{R}^d$ and $\mathbb{R}^{d-1}$, respectively. The scaling assumption implies that the number of edges and faces in each elemental boundary is uniformly bounded over the whole mesh family $\mathcal{T}$.

In the following C will denote a generic positive constant independent of the mesh diameter h (possibly dependent on ϱ) and that may change at each occurrence, and $\lesssim$ will denote a bound up to C.

3.2. Basic setting

Throughout the paper, $\mathbb{P}_\ell(\omega)$ denotes the space of polynomials of degree up to ℓ for any integer number $\ell \geq 0$ on the bounded connected subset ω of $\mathbb{R}^\nu$ with $\nu = 1, 2, 3$. The polynomial space $\mathbb{P}_\ell(\omega)$ is finite dimensional and we denote its dimension by $\pi_{\ell,\nu}$. It holds that

$$\pi_{\ell,1} = \ell + 1\,, \qquad \pi_{\ell,2} = \frac{(\ell+1)(\ell+2)}{2}\,, \qquad \pi_{\ell,3} = \frac{(\ell+1)(\ell+2)(\ell+3)}{6}. \tag{3.1}$$

We also conventionally take $\mathbb{P}_{-1}(\omega) = \{0\}$ and $\pi_{-1,\nu} = 0$. We denote by $\Pi_\ell^{0,P} : L^2(P) \to \mathbb{P}_\ell(P)$ for $\ell \geq 0$ the L^2-orthogonal projection onto the polynomial space $\mathbb{P}_\ell(P)$ and by $\Pi_\ell^{0,\sigma} : L^2(\sigma) \to \mathbb{P}_\ell(\sigma)$ for $\ell \geq 0$ the L^2-orthogonal projection onto the polynomial space $\mathbb{P}_\ell(\sigma)$. We now introduce the broken Sobolev space for any $s > 0$

$$H^s(\Omega_h) = \prod_{P\in\Omega_h} H^s(P) = \left\{ v \in L^2(\Omega) \,:\, v_{|P} \in H^s(P) \right\},$$

and define the broken H^s-norm

$$\|v\|_{s,h}^2 = \sum_{P\in\Omega_h} \|v\|_{s,P}^2 \qquad \text{for all } v \in H^s(\Omega_h), \tag{3.2}$$

and for $s = 1$ the broken H^1-seminorm

$$|v|_{1,h}^2 = \sum_{P\in\Omega_h} \|\nabla v\|_{0,P}^2 \qquad \text{for all } v \in H^s(\Omega_h). \tag{3.3}$$

Let $\sigma \subset \partial P_\sigma^+ \cap \partial P_\sigma^-$ be the internal side shared by elements P_σ^+ and P_σ^-, and v a function that belongs to $H^1(\Omega_h)$. We denote the traces of v on σ from the interior of elements $P_\sigma^\pm$ by $v_\sigma^\pm$, and the unit normal vectors to σ pointing from $P_\sigma^\pm$ to $P_\sigma^\mp$ by $\mathbf{n}_\sigma^\pm$. Then, we introduce the jump operator $[\![\, v \,]\!] = v_\sigma^+ \mathbf{n}_\sigma^+ + v_\sigma^- \mathbf{n}_\sigma^-$ at each internal side $\sigma \in \mathcal{S}_h^0$ and $[\![\, v \,]\!] = v_\sigma \mathbf{n}_\sigma$ at each boundary side $\sigma \in \mathcal{S}_h^\partial$.

Let $k \geq 1$ the polynomial degree of accuracy of the method. The nonconforming space $H^{1,nc}(\Omega_h; k)$ is the subspace of the broken Sobolev space $H^1(\Omega_h)$ defined as

$$H^{1,nc}(\Omega_h; k) = \left\{ v \in H^1(\Omega_h) \,:\, \int_\sigma [\![\, v \,]\!] \cdot \mathbf{n}_\sigma \, q \, \mathrm{d}\sigma = 0 \;\; \forall\, q \in \mathbb{P}_{k-1}(\sigma),\; \forall \sigma \in \mathcal{S}_h \right\}. \tag{3.4}$$

Since $[\![\, v \,]\!] = 0$ on any internal mesh side whenever v belongs to $H^1(\Omega)$, it is clear that $H_0^1(\Omega) \subset H^{1,nc}(\Omega_h; k)$.

Hereafter, we consider the extension of the bilinear form $a(\cdot,\cdot)$ in (2.3) to the space $H^1(\Omega_h)$, which is given by splitting it as sum of local terms:

$$a : H^1(\Omega_h) \times H^1(\Omega_h) \to \mathbb{R} \quad \text{with} \qquad a(u,v) = \sum_{P\in\Omega_h} a^P(u,v) := \sum_{P\in\Omega_h} \int_P \nabla u \cdot \nabla v \, \mathrm{d}P \quad \text{for all } u, v \in H^1(\Omega_h). \tag{3.5}$$

From the Poincaré-Friedrichs inequality (see for instance [21]), it is straightforward to check that $|\cdot|_{1,h}$ is actually a norm on $H^{1,nc}(\Omega_h; k)$, although it is only a seminorm for the discontinuous functions of $H^1(\Omega_h)$. Moreover, according to [7], let $u \in V$ be the solution to problem (2.5) and $v \in H^{1,nc}(\Omega_h; k)$ then it holds that

$$\mathcal{N}_h(u,v) := a(u,v) - b(g,v) = \sum_{\sigma\in\mathcal{S}_h} \int_\sigma \nabla u \cdot [\![\, v \,]\!] \, \mathrm{d}\sigma. \tag{3.6}$$

The quantity $\mathcal{N}_h(u,v)$ is called the *conformity error*. We now consider the following estimate for the term measuring the nonconformity. This Lemma generalises the result of Lemma 4.1 from [7] since its proof does not require any H^2-regularity assumption.

Lemma 3.2. *Under the assumption* **(A0)**, *let* $u \in H^{1+r}(\Omega)$ *with* $r > \frac{1}{2}$ *be the solution to Problem* (2.5). *Let* $v \in H^{1,nc}(\Omega_h;k)$ *as defined in* (3.4). *Then, there exists a constant* $C > 0$ *depending only on the polynomial degree* k *and the mesh regularity constant* ϱ *such that*

$$|\mathcal{N}_h(u,v)| \leq Ch^t|u|_{1+r}|v|_{1,h} \tag{3.7}$$

where $t = \min\{k, r\}$ *and* $\mathcal{N}_h(u,v)$ *is defined in* (3.6).

Proof. The proof of this Lemma follows the same lines as that in Lemma 4.1 of [7], except for the last step of the inequality chain (4.4) where we apply the trace inequality that we will state later in (3.17). □

3.3. Local and global nonconforming virtual element space

We construct the local nonconforming virtual element space by resorting to the so-called *enhancement strategy* originally devised in [3] for the conforming VEM and later extended to the nonconforming VEM in [31]. To this end, on every polytopal cell $P \in \Omega_h$ we first define the finite dimensional functional space

$$\widetilde{V}_k^h(P) = \left\{ v_h \in H^1(P) \,:\, \frac{\partial v_h}{\partial \mathbf{n}} \in \mathbb{P}_{k-1}(\sigma) \quad \forall\, \sigma \subset \partial P, \quad \Delta v_h \in \mathbb{P}_k(P) \right\}. \tag{3.8}$$

We notice that the space $\widetilde{V}_k^h(P)$ clearly contains the polynomials of degree k. We consider the set of linear operators from $\widetilde{V}_k^h(P)$ to $\mathbb{R}$ that for every virtual function v_h of $\widetilde{V}_k^h(P)$ provide:

(D1) the moments of v_h of order up to $k-1$ on each $(d-1)$-dimensional side $\sigma \in \partial P$:

$$\frac{1}{|\sigma|}\int_\sigma v_h\, p_{k-1}\,\mathrm{d}\sigma \qquad \text{for all } p_{k-1} \in \mathbb{P}_{k-1}(\sigma) \text{ and for all } \sigma \in \partial P; \tag{3.9}$$

(D2) the moments of v_h of order up to $k-2$ on P:

$$\frac{1}{|P|}\int_P v_h\, p_k\,\mathrm{d}P \qquad \text{for all } p_k \in \mathbb{P}_k(P). \tag{3.10}$$

Finally, we introduce the elliptic projection operator $\Pi_k^{\nabla,P} : \widetilde{V}_k^h(P) \to \mathbb{P}_k(P)$ defined for all $v_h \in \widetilde{V}_k^h(P)$ by

$$\begin{cases} \displaystyle\int_P \nabla\Pi_k^{\nabla,P} v_h \cdot \nabla q_k\,\mathrm{d}P = \int_P \nabla v_h \cdot \nabla q_k\,\mathrm{d}P \qquad \text{for all } q_k \in \mathbb{P}_k(P), \\ \displaystyle\int_{\partial P} (\Pi_k^{\nabla,P} v_h - v_h)\,\mathrm{d}\sigma = 0. \end{cases}$$

As proved in [31], the polynomial projection $\Pi_k^{\nabla,P} v_h$ is exactly computable using only the values from the linear operators **(D1)** and **(D2)**. Furthermore, $\Pi_k^{\nabla,P}$ is a polynomial-preserving operator, *i.e.*, $\Pi_k^{\nabla,P} q_k = q_k$ for every $q_k \in \mathbb{P}_k(P)$.

We are now ready to introduce the *local nonconforming virtual element space of order* k on the polytopal element P, which is the subspace of $\widetilde{V}_k^h(P)$ defined as follow:

$$V_k^h(P) = \left\{ v \in \widetilde{V}_k^h(P) \quad \text{such that} \quad (v_h - \Pi_k^{\nabla,P} v_h,\, \widehat{q}_k)_P = 0 \;\; \forall \widehat{q}_k \in \mathbb{P}_k(P) \setminus \mathbb{P}_{k-2}(P) \right\} \tag{3.11}$$

where $\mathbb{P}_k(P)\setminus\mathbb{P}_{k-2}(P)$ denotes the polynomials in $\mathbb{P}_k(P)$ that are L^2-orthogonal to all polynomials of $\mathbb{P}_{k-2}(P)$. The space $V_k^h(P)$ has the two important properties that we outline below [7,31]:

– it still contains the space of polynomials of degree at most k;

– the dimension of $V_k^h(P)$ is
$$\dim(V_k^h(P)) = \pi_{k-2,d} + n_{\sigma,P}\,\pi_{k-1,d} \tag{3.12}$$
where $n_{\sigma,P}$ is the number of sides of P;
– the linear operators **(D1)** and **(D2)** constitute a set of *degrees of freedom* (DoFs) for $V_k^h(P)$;
– the DoFs **(D1)** and **(D2)** allow us to compute exactly
$$\Pi_k^{\nabla,P}\colon V_k^h(P) \to \mathbb{P}_k(P), \qquad \Pi_k^{0,P}\colon V_k^h(P) \to \mathbb{P}_k(P)$$
in the sense that, given any $v_h \in V_k^h(P)$, we are able to compute the polynomials $\Pi_k^{\nabla,P} v_h$ and $\Pi_k^{0,P} v_h$ only using, as unique information, the degree of freedom values **(D1)** and **(D2)** of v_h.

The *global nonconforming virtual element space* V_k^h *of order* $k \geq 1$ *subordinate to the mesh* Ω_h is obtained by gluing together the elemental spaces $V_k^h(P)$. The formal definition reads as:
$$V_k^h := \left\{ v_h \in H^{1,nc}(\Omega_h; k) \,:\, v_{h|P} \in V_k^h(P) \;\; \forall P \in \Omega_h \right\}. \tag{3.13}$$
A set of degrees of freedom for V_k^h is given by collecting the local DoFs **(D1)** and **(D2)** for all the mesh elements. The dimension of V_k^h is
$$\dim(V_k^h) = N_P\,\pi_{k-2,d} + N_\sigma\,\pi_{k-1,d} \tag{3.14}$$
where N_P are N_σ are respectively the number of elements and internal sides in the decomposition Ω_h.

Remark 3.3. The H^1-conforming virtual element counterpart $V_k^{h,\mathrm{conf}}(P)$ of space $V_k^h(P)$ has dimension [3, 9, 31]
$$\dim(V_k^{h,\mathrm{conf}}(P)) = \begin{cases} \pi_{k-2,2} + n_{e,P}\,\pi_{k-2,1} + n_{v,P} & \text{for } d = 2, \\ \pi_{k-2,3} + n_{f,P}\,\pi_{k-2,2} + n_{e,P}\,\pi_{k-1,1} + n_{v,P} & \text{for } d = 3, \end{cases} \tag{3.15}$$
where $n_{f,P}$ (resp., $n_{e,P}$ and $n_{v,P}$) denotes the number of faces (resp., edges and vertexes) in P.

For the two-dimensional case, a careful inspection of (3.1), (3.12) and (3.15) shows that the conforming and nonconforming local spaces have the same dimension. Concerning the comparison between the global spaces $V_k^{h,\mathrm{conf}}$ and V_k^h, recalling the Euler formula
$$N_v - N_e + N_P = 1$$
where N_P (resp., N_e and N_v) is the number of elements (resp., internal edges and vertexes) in the decomposition Ω_h, it holds that
$$\dim(V_k^{h,\mathrm{conf}}) = \dim(V_k^h) - N_P + 1.$$

For the three-dimensional case the analysis is more involved. At practical level the comparison depends on the geometry of the element: if P has a large number of edges, the conforming approximation yields a greater number of DoFs.

However we recall that a possible recipe to reduce the number of DoFs for conforming VEM is shown in [13, 14], where the *serendipity* approach is exploited.

3.4. Approximation properties

Both for completeness of exposition and future reference in the paper, we briefly summarize the local approximation properties by polynomial functions and functions in the virtual nonconforming space. We omit here any details about the derivation of these estimates and refer the interested readers to References [3, 7, 9, 16, 22, 23, 28, 34, 39].

Local polynomial approximations. On a given element $P \in \Omega_h$, let $v \in H^s(P)$ with $1 \le s \le k+1$. Under mesh assumptions **(A0)**, there exists a piecewise polynomial approximation v_π that is of degree k on each element, such that

$$\|v - v_\pi\|_{0,P} + h_P |v - v_\pi|_{1,P} \le C h_P^s |v|_{s,P}, \tag{3.16}$$

for some constant $C > 0$ that depends only on the polynomial degree k and the mesh regularity constant ϱ.

An instance of such a local polynomial approximation is provided by the L^2-projection $\Pi_k^{0,P} v$ onto the local polynomial space $\mathbb{P}_k(P)$, which satisfies the (optimal) error bound (3.16) (see also [39], Lem. 1.58).

Trace inequality. Under the assumption **(A0)**, consider the internal side $\sigma \in \mathcal{S}_h^0$ and let $P_\sigma^\pm$ be the two elements sharing σ, so that $\sigma \subset \partial P_\sigma^+ \cap \partial P_\sigma^-$. Let $\Omega_\sigma = P_\sigma^+ \cup P_\sigma^-$. Then, the following trace inequality (see [39], Lem. 1.49 for the case of H^1-regularity, and [41], Lem. 7.2 for the minimal regularity case H^m with $m > \frac{1}{2}$) holds for every $v \in H^m(\Omega_\sigma), m > \frac{1}{2}$

$$\|v\|_{0,\sigma} \le C h_\sigma^{-\frac{1}{2}} \|v\|_{0,\Omega_\sigma} + C h_\sigma^{m-\frac{1}{2}} |v|_{m,\Omega_\sigma}, \tag{3.17}$$

where the constant C depends only on the mesh regularity constant ϱ.

Moreover, for every $v \in H^s(\Omega_h)$ with $\frac{1}{2} < s \le k+1$, combining the L^2-projection approximation property with (3.17) the following useful error estimate holds (see [39], Lem. 1.59)

$$\|v - \Pi_k^{0,\sigma} v\|_{0,\sigma} \le C h_\sigma^{s-\frac{1}{2}} |v|_{s,\Omega_\sigma}. \tag{3.18}$$

The same estimate holds also for the boundary sides $\sigma \in \mathcal{S}_h^\partial$ by taking $\Omega_\sigma = P$, the element to which σ belongs.

Interpolation error. Under mesh regularity assumptions **(A0)**, we can define an interpolation operator in V_k^h having optimal approximation properties (see [28], Thm. 11). Therefore, for every $v \in H^s(\Omega)$ with $1 \le s \le k+1$, there exists $v^I \in V_k^h$ such that

$$\|v - v^I\|_0 + h|v - v^I|_1 \le C h^s |v|_s, \tag{3.19}$$

where $C > 0$ depends only on the polynomial degree k and the mesh regularity constant ϱ.

4. The virtual element discretization

This section briefly reviews the nonconforming virtual element discretization of the source problem and its extension to the eigenvalue problem.

4.1. The virtual element discretization of the source problem

The goal of the present section is to introduce the virtual element discretization of the source problem (2.5). According to [7, 42], we define a suitable discrete bilinear form $a_h(\cdot,\cdot)$ approximating the continuous gradient-gradient form $a(\cdot,\cdot)$, whereas for what concerns the bilinear form $b(\cdot,\cdot)$ we propose two possible discretizations, hereafter denoted by $b_h(\cdot,\cdot)$ and $\widetilde{b}_h(\cdot,\cdot)$.

The discrete bilinear form $a_h(\cdot,\cdot)$ is the sum of elemental contributions

$$a_h(u_h, v_h) = \sum_{P \in \Omega_h} a_h^P(u_h, v_h), \tag{4.1}$$

where

$$a_h^P(u_h, v_h) = a^P(\Pi_k^{\nabla,P} u_h, \Pi_k^{\nabla,P} v_h) + S^P\Big((I - \Pi_k^{\nabla,P})u_h, (I - \Pi_k^{\nabla,P})v_h\Big) \qquad \text{for all } v_h \in V_k^h(P) \tag{4.2}$$

and $S^P(\cdot,\cdot)$ denotes any symmetric positive definite bilinear form on the element P for which there exist two positive uniform constants c_* and c^* such that

$$c_* a^P(v_h, v_h) \leq S^P(v_h, v_h) \leq c^* a^P(v_h, v_h) \quad \text{for all } v_h \in V_k^h(P) \cap \ker(\Pi_k^{\nabla,P}). \tag{4.3}$$

This requirement implies that $S^P(\cdot,\cdot)$ scales like $a^P(\cdot,\cdot)$, namely $S^P(\cdot,\cdot) \simeq h_P^{d-2}$.
The choice of the discrete form $a_h(\cdot,\cdot)$ is driven by the need to satisfy the following properties:

– *k-consistency*: for all $v_h \in V_k^h(P)$ and for all $q \in \mathbb{P}_k(P)$ it holds

$$a_h^P(v_h, q) = a^P(v_h, q); \tag{4.4}$$

– *stability*: there exists two positive constants α_*, α^*, independent of h and of P, such that

$$\alpha_* a^P(v_h, v_h) \leq a_h^P(v_h, v_h) \leq \alpha^* a^P(v_h, v_h) \quad \text{for all } v_h \in V_k^h(P). \tag{4.5}$$

In particular, the first term in (4.2) ensures the k-consistency of the method and the second one its stability, *cf.* [7].

For what concerns the right hand side $b(\cdot,\cdot)$, following the setting in [42], we introduce two possible approximated bilinear forms.

Non–stabilized bilinear form. In the first choice, we consider the bilinear form $b_h(\cdot,\cdot)$, which satisfies the k-consistency property but not the stability property (extending to $b_h(\cdot,\cdot)$ the definitions in (4.4) and (4.5)). Let us split the right-hand side $b_h(\cdot,\cdot)$ with the sum of local contributions:

$$b_h(f, v_h) = \sum_{P\in\Omega_h} b_h^P(f, v_h). \tag{4.6}$$

Then, we define

$$b_h^P(f, v_h) = b^P(\Pi_k^{0,P} f, v_h) \qquad \text{for all } v_h \in V_k^h(P). \tag{4.7}$$

We observe that each local term is fully computable for any functions $f \in L^2(\Omega)$ and v_h in V_k^h since

$$b_h(f, v_h) = \sum_{P\in\Omega_h} \int_P (\Pi_k^{0,P} f) v_h \,\mathrm{d}P = \sum_{P\in\Omega_h} \int_P f(\Pi_k^{0,P} v_h) \,\mathrm{d}P,$$

and $\Pi_k^{0,P} v_h$ is computable (exactly) from the DoFs $\boldsymbol{(D)}$ of v_h (*cf.* Property (i)). Moreover, by definition of L^2-projection $\Pi_k^{0,P}$, it is straightforward to check that

$$b_h^P(f, v_h) = b^P(\Pi_k^{0,P} f, \Pi_k^{0,P} v_h) \qquad \text{for all } v_h \in V_k^h(P). \tag{4.8}$$

We estimate the approximation error of the right-hand side by using the Cauchy-Schwarz inequality twice and estimate (3.16), after noting that $v_{h|P} \in H^1(P)$ and $\Pi_0^{0,P} v_h$ is orthogonal to $f - \Pi_k^{0,P} f$:

$$\begin{aligned} |b(f, v_h) - b_h(f, v_h)| &\leq \sum_{P\in\Omega_h} \left| b^P(f - \Pi_k^{0,P} f, v_h) \right| = \sum_{P\in\Omega_h} \left| b^P((I - \Pi_k^{0,P}) f, (I - \Pi_0^{0,P}) v_h) \right| \\ &\leq \sum_{P\in\Omega_h} \|(I - \Pi_k^{0,P}) f\|_{0,P} \|(I - \Pi_0^{0,P}) v_h\|_{0,P} \\ &\lesssim \sum_{P\in\Omega_h} h_P \|(I - \Pi_k^{0,P}) f\|_{0,P} |v_h|_{1,P} \lesssim h \left(\sum_{P\in\Omega_h} \|(I - \Pi_k^{0,P}) f\|_{0,P}^2 \right)^{1/2} |v_h|_{1,h}. \end{aligned} \tag{4.9}$$

In the light of (4.1) and (4.6), the virtual element discretization of source problem (2.5) reads as

$$\begin{cases} \text{find } u_h^s \in V_k^h & \text{such that} \\ a_h(u_h^s, v_h) = b_h(f, v_h) & \text{for all } v_h \in V_k^h. \end{cases} \tag{4.10}$$

Stabilized bilinear form. The second approximation of the bilinear form in (2.4) is inspired by the definition of the virtual bilinear form a_h. In order to distinguish the two formulations, we denote the stabilized bilinear form by $\widetilde{b}_h(\cdot,\cdot)$. As usual, we first decompose $\widetilde{b}_h(\cdot,\cdot)$ into the sum of local contributions:

$$\widetilde{b}_h(f, v_h) = \sum_{P\in\Omega_h} \widetilde{b}_h^P(f, v_h)\,, \tag{4.11}$$

and, then, we define

$$\widetilde{b}_h^P(f, v_h) = b^P(\Pi_k^{0,P} f, \Pi_k^{0,P} v_h) + \widetilde{S}^P\Big((I-\Pi_k^{0,P})f, (I-\Pi_k^{0,P})v_h\Big) \qquad \text{for all } v \in V_k^h(P), \tag{4.12}$$

where $\widetilde{S}^P$ is any positive definite bilinear form on the element P such that there exist two uniform positive constants β_* and β^* such that

$$\beta_* b^P(v,v) \le \widetilde{S}^P(v,v) \le \beta^* b(v,v) \quad \text{for all } v \in V_k^h(P) \cap \ker(\Pi_k^{0,P}). \tag{4.13}$$

We notice that the bilinear form $\widetilde{b}_h^P$ defined above satisfies both the k-consistency and the stability property.

Remark 4.1. In analogy with the condition on the form $S^P(\cdot,\cdot)$, we require that the form $\widetilde{S}^P(\cdot,\cdot)$ scales like $b^P(\cdot,\cdot)$, that is $\widetilde{S}^P(\cdot,\cdot) \simeq h^d$.

By definition (4.12) and from inequalities in (4.13), using similar computations as in (4.9), for all $f \in L^2(\Omega)$ and for all $v_h \in V_k^h(P)$ it holds that

$$\begin{aligned} |b(f,v_h) - \widetilde{b}_h(f,v_h)| &\le \sum_{P\in\Omega_h} \Big(\big|b^P(f-\Pi_k^{0,P}f, v_h)\big| + \widetilde{S}^P\Big((I-\Pi_k^{0,P})f, (I-\Pi_k^{0,P})v_h\Big)\Big) \\ &\le \sum_{P\in\Omega_h} \Big(\big|b^P((I-\Pi_k^{0,P})f, (I-\Pi_0^{0,P})v_h)\big| + \beta^* \|(I-\Pi_k^{0,P})f\|_0 \|(I-\Pi_k^{0,P})v_h\|_0\Big) \\ &\le \sum_{P\in\Omega_h} (1+\beta^*) \|(I-\Pi_k^{0,P})f\|_{0,P} \|(I-\Pi_0^{0,P})v_h\|_{0,P} \\ &\lesssim \sum_{P\in\Omega_h} h_P \|(I-\Pi_k^{0,P})f\|_{0,P} |v_h|_{1,P} \lesssim h \left(\sum_{P\in\Omega_h} \|(I-\Pi_k^{0,P})f\|_{0,P}^2 \right)^{1/2} |v_h|_{1,h}. \end{aligned} \tag{4.14}$$

From (4.1) and (4.11), the second formulation reads as:

$$\begin{cases} \text{find } u_h^s \in V_k^h & \text{such that} \\ a_h(u_h^s, v_h) = \widetilde{b}_h(f, v_h) & \text{for all } v_h \in V_k^h. \end{cases} \tag{4.15}$$

The well-posedness of the discrete source problems (4.10) and (4.15) stem from the the coercivity and the continuity of the bilinear form $a_h(\cdot,\cdot)$ (*cf.* (4.5)), and from the continuity of the discrete forms $b_h(\cdot,\cdot)$ and $\widetilde{b}_h(\cdot,\cdot)$.

Following the same arguments as in [7] but with $\Pi_k^{0,P} f$ for $k \ge 1$ instead of $\Pi_{k-2}^{0,P} f$, we derive the error estimates in the H^1-norm and L^2-norm that we summarize in the following theorem for next reference in the paper.

We can state the following optimal error estimates between the solution to the continuous and discrete source problems (4.10) and (4.15).

Theorem 4.2. *Under the assumptions* ***(A0)****, let* $u^s \in H^{1+r}(\Omega)$ *with regularity index* $r > \frac{1}{2}$ *be the solution to* (2.5) *with* $f \in L^2(\Omega)$.

Let u_h^s *and* $\widetilde{u}_h^s \in V_k^h$ *be respectively the solutions to the nonconforming virtual element method* (4.10) *and* (4.15). *Let* $v_h \in \{u_h^s, \widetilde{u}_h^s\}$, *then we have the following error estimates*

– H^1*-error estimate:*

$$|u^s - v_h|_{1,h} \lesssim h^t |u^s|_{1+r} + h \left(\sum_{P \in \Omega_h} \|(I - \Pi_k^{0,P}) f\|_{0,P}^2 \right)^{1/2}$$

– L^2*-error estimate (for a convex* Ω*):*

$$\|u^s - v_h\|_0 \lesssim h^{t+1} |u^s|_{1+r} + h^2 \left(\sum_{P \in \Omega_h} \|(I - \Pi_k^{0,P}) f\|_{0,P}^2 \right)^{1/2}$$

with $t = min(k, r)$.

The proofs of these estimates are omitted as they are almost identical to those of Theorems 4.3 and 4.5 from [7]. The only difference is that here the forcing term f is approximated in each element by the orthogonal projection onto polynomials of degree k instead of $\overline{k} = \max(k-2, 0)$ (see estimates (4.9) and (4.14)). Note, indeed, that in the L^2-estimate of Theorem 4.5 from [7], the term that depends on the approximation of f is given by

$$(h_P^2 + h_P^{\overline{k}+1}) \|(I - \Pi_k^{0,P}) f\|_{0,P} = \begin{cases} (h_P^2 + h_P) \|(I - \Pi_k^{0,P}) f\|_{0,P} & \text{for } k = 1, 2, \\ h_P^2 \|(I - \Pi_k^{0,P}) f\|_{0,P} & \text{for } k \geq 3. \end{cases}$$

The difference in the coefficients is a consequence of the orthogonality of $(I - \Pi_k^{0,P}) f$ to the polynomials of degree k instead of $\overline{k}$.

Remark 4.3. We observe that if the load term f is an eigenfunction of problem (2.2), then f solves the continuous source problem (2.5) with datum λf and thus, thanks to the regularity result (2.6), it belongs to $H^{1+r}(\Omega)$ and $|f|_{1+r} \leq C \|f\|_0$. Then, the *a priori* error estimates in Theorem 4.2 reduce to

– H^1-error estimate:

$$|u^s - v_h|_{1,h} \lesssim h^t |u^s|_{1+r} + h \left(\sum_{P \in \Omega_h} \|(I - \Pi_k^{0,P}) f\|_{0,P}^2 \right)^{1/2} \lesssim h^t |u^s|_{1+r} \lesssim h^t \|f\|_0 \lesssim h^t,$$

– L^2-error estimate:

$$\|u^s - v_h\|_0 \lesssim h^{t+1} |u^s|_{1+r} + h^2 \left(\sum_{P \in \Omega_h} \|(I - \Pi_k^{0,P}) f\|_{0,P}^2 \right)^{1/2} \lesssim h^{t+1} |u^s|_{1+r} \lesssim h^{t+1} \|f\|_0 \lesssim h^{t+1},$$

since

$$\|(I - \Pi_k^{0,P}) f\|_{0,P} \lesssim h_P^{\min\{k+1, 1+r\}} |f|_{1+r,P} \lesssim h_P^{t+1} \|f\|_{0,P}.$$

Remark 4.4. In [7] it is proved that the discrete problem (4.10) is well-posed by taking, in the definition of the discrete bilinear form $b_h(\cdot,\cdot)$, instead of $\Pi_k^{0,P} f$, $\Pi_{k-2}^{0,P} f$ for $k \geq 2$ and a first-order approximation of $\Pi_0^{0,P} f$ for $k = 1$. However, in the definition of the discrete bilinear forms $b_h(\cdot,\cdot)$ and $\widetilde{b}_h(\cdot,\cdot)$, we project onto the space $\mathbb{P}_k(P)$. This choice does not provide a better convergence rate, due to the k-consistency property, but it has been numerically observed that it gives more accurate results.

4.2. The virtual element discretization of the eigenvalue problem.

In the light of the nonconforming virtual element method (4.10) and (4.15) introduced in the previous section, following [42], we consider two different discretizations of the eigenvalue problem (2.2). The first formulation in inspired to the source problem (4.10), and uses definition (4.6). We formulate the virtual element approximation of (2.2) as:

$$\begin{cases} \text{find } (\lambda_h,\, u_h) \in \mathbb{R} \times V_k^h & \text{with } \|u_h\|_0 = 1 \text{ such that} \\ a_h(u_h, v_h) = \lambda_h\, b_h(u_h, v_h) & \text{for all } v_h \in V_k^h. \end{cases} \tag{4.16}$$

The second formulation is inspired to the virtual source problem (4.15) and uses definition (4.11). We formulate the second approximation of problem (2.2) as:

$$\begin{cases} \text{find } (\lambda_h,\, u_h) \in \mathbb{R} \times V_k^h & \text{with } \|u_h\|_0 = 1 \text{ such that} \\ a_h(u_h, v_h) = \lambda_h\, \widetilde{b}_h(u_h, v_h) & \text{for all } v_h \in V_k^h. \end{cases} \tag{4.17}$$

5. Spectral approximation for compact operators

In this section, we briefly recall some spectral approximation results that can be deduced from [8, 20, 44]. For more general results, we refer to the original papers. Before stating the spectral approximation results, we introduce a natural compact operator associated with problem (2.2) and its discrete counterpart, and we recall their connection with the eigenmode convergence.

We associate problem (2.2) with its solution operator $T \in \mathcal{L}(L^2(\Omega))$, which is the bounded linear operator $T : L^2(\Omega) \to L^2(\Omega)$ mapping the forcing term f to $u^s =: Tf$:

$$\begin{cases} Tf \in V & \text{such that} \\ a(Tf, v) = b(f, v) & \text{for all } v \in V. \end{cases}$$

Operator T is self-adjoint and positive definite with respect to the inner products $a(\cdot,\cdot)$ and $b(\cdot,\cdot)$ on V, and compact due to the compact embedding of $H^1(\Omega)$ in $L^2(\Omega)$.

Similarly, we associate problem (4.10) with its solution operator $T_h \in \mathcal{L}(L^2(\Omega))$ and problem (4.15) with its solution operator $\widetilde{T}_h \in \mathcal{L}(L^2(\Omega))$. The former is the bounded linear operator mapping the forcing term f to $u_h^s =: T_h f$ and satisfies:

$$\begin{cases} T_h f \in V_k^h & \text{such that} \\ a_h(T_h f, v_h) = b_h(f, v_h) & \text{for all } v_h \in V_k^h. \end{cases}$$

The latter is the bounded linear operator mapping the forcing term f to $\widetilde{u}_h^s =: \widetilde{T}_h f$ and satisfies:

$$\begin{cases} \widetilde{T}_h f \in V_k^h & \text{such that} \\ a_h(\widetilde{T}_h f, v_h) = \widetilde{b}_h(f, v_h) & \text{for all } v_h \in V_k^h. \end{cases}$$

Both operators T_h and $\widetilde{T}_h$ are self-adjoint and positive definite with respect to the inner products $a_h(\cdot,\cdot)$, $b_h(\cdot,\cdot)$ and $a_h(\cdot,\cdot)$, $\widetilde{b}_h(\cdot,\cdot)$. They are also compact since their ranges are finite dimensional.

The eigensolutions of the continuous problem (2.2) and the discrete problems (4.16) and (4.17) are respectively related to the eigenmodes of the operators T, T_h, and $\widetilde{T}_h$. In particular, (λ, u) is an eigenpair of problem (2.2) if and only if $Tu = (1/\lambda)u$, *i.e.* $(\frac{1}{\lambda}, u)$ is an eigenpair for the operator T, and analogously for problems (4.16) and (4.17) and operators T_h and $\widetilde{T}_h$. By virtue of this correspondence, the convergence analysis can be derived from the spectral approximation theory for compact operators. In the rest of this section we refer only to operators T and $\widetilde{T}_h$. Identical considerations hold for operators T and T_h and we omit them for brevity.

A sufficient condition for the correct spectral approximation of a compact operator T is the uniform convergence to T of the family of discrete operators $\{\widetilde{T}_h\}_h$ (see [20], Prop. 7.4, *cf.* also [8]):

$$\|T - \widetilde{T}_h\|_{\mathcal{L}(L^2(\Omega))} \to 0, \quad \text{as } h \to 0, \tag{5.1}$$

or, equivalently,

$$\|(T - \widetilde{T}_h)f\|_0 \leq C\rho(h)\|f\|_0 \quad \forall f \in L^2(\Omega), \tag{5.2}$$

with $\rho(h)$ tending to zero as h goes to zero. Condition(5.2) usually follows from *a priori* estimates with no additional regularity assumption on f. Besides the convergence of the eigenmodes, condition (5.1), or the equivalent condition (5.2), implies that no spurious eigenvalues may pollute the spectrum. In fact,

(i) each continuous eigenvalue is approximated by a number of discrete eigenvalues (counted with their multiplicity) that corresponds exactly to its multiplicity;
(ii) each discrete eigenvalue approximates a continuous eigenvalue.

Condition (5.1) does not provide any indication on the approximation rate. It is common to split the convergence analysis for eigenvalue problems into two steps: first, the convergence and the absence of spurious modes is studied; then, suitable convergence rates are proved. We now report the main results about the spectral approximation for compact operators. (*cf.* [8], Thms. 7.1–7.4; see also [20], Thms. 9.3–9.7), which deal with the order of convergence of eigenvalues and eigenfunctions.

Theorem 5.1. *Let the uniform convergence (5.1) hold true. Let μ be an eigenvalue of T, with multiplicity m, and denote the corresponding eigenspace by E_μ. Then, exactly m discrete eigenvalues $\widetilde{\mu}_{1,h}, \ldots, \widetilde{\mu}_{m,h}$ (repeated according to their respective multiplicities) converges to μ. Moreover, let $\widetilde{E}_{\mu,h}$ be the direct sum of the eigenspaces corresponding to the discrete eigenvalues $\widetilde{\mu}_{1,h}, \cdots, \widetilde{\mu}_{m,h}$ converging to μ. Then*

$$\delta(E_\mu, \widetilde{E}_{\mu,h}) \leq C\|(T - \widetilde{T}_h)_{|E_\mu}\|_{\mathcal{L}(L^2(\Omega))}, \tag{5.3}$$

with

$$\delta(E_\mu, \widetilde{E}_{\mu,h}) = \max(\hat{\delta}(E_\mu, \widetilde{E}_{\mu,h}), \hat{\delta}(\widetilde{E}_{\mu,h}, E_\mu))$$

where, in general,

$$\hat{\delta}(U, W) = \sup_{u \in U, \|u\|_0 = 1} \inf_{w \in W} \|u - w\|_0$$

denotes the gap between U, $W \subseteq L^2(\Omega)$.

Concerning the eigenvalue approximation error, we recall the following result.

Theorem 5.2. *Let the uniform convergence (5.1) hold true. Let $\phi_1, \ldots, \phi_m$ be a basis of the eigenspace E_μ of T corresponding to the eigenvalue μ. Then, for $i = 1, \ldots, m$*

$$|\mu - \widetilde{\mu}_{i,h}| \leq C\Big(\sum_{j,k=1}^{m} |b((T - \widetilde{T}_h)\phi_k, \phi_j)| + \|(T - \widetilde{T}_h)_{|E_\mu}\|^2_{\mathcal{L}(L^2(\Omega))} \Big), \tag{5.4}$$

where $\widetilde{\mu}_{1,h}, \ldots, \widetilde{\mu}_{m,h}$ are the m discrete eigenvalues converging to μ repeated according to their multiplicities.

6. Convergence analysis and error estimates

In this section we study the convergence of the discrete eigenmodes provided by the VEM approximation to the continuous ones. We will consider the stabilized discrete formulation (4.17). The analysis can be easily applied to the non–stabilized one (4.16).

6.1. Convergence analysis for the stabilized formulation

In the case of the first VEM approximation of problem (2.2), which uses the stabilized form $\widetilde{b}_h(\cdot,\cdot)$, the uniform convergence of the sequence of operators $\widetilde{T}_h$ to T directly stems from the L^2-*a priori* error estimate of Theorem 4.2.

Theorem 6.1. *The family of operators $\widetilde{T}_h$ associated with problem (4.15) converges uniformly to the operator T associated with problem (2.5), that is,*

$$\|T-\widetilde{T}_h\|_{\mathcal{L}(L^2(\Omega))}\to 0 \quad \textit{for} \quad h\to 0. \tag{6.1}$$

Proof. Let u^s and $\widetilde{u}_h^s$ be the solutions to the continuous and the discrete source problems (2.5) and (4.15), respectively. The L^2-estimate of Theorem 4.2 with $f\in L^2(\Omega)$ and the stability condition (2.6) imply that

$$\|u^s-\widetilde{u}_h^s\|_0 \lesssim h^{\min(t+1,2)}\|f\|_0$$

with $t=\min(k,r)$, $k\geq 1$ being the order of the method and r at least in $(1/2,1]$ being the regularity index of the solution $u^s\in H^{1+r}(\Omega)$ to the continuous source problem in equation (2.6). From this inequality it follows that

$$\|T-\widetilde{T}_h\|_{\mathcal{L}(L^2(\Omega))}=\sup_{f\in L^2(\Omega)}\frac{\|Tf-\widetilde{T}_hf\|_0}{\|f\|_0}=\sup_{f\in L^2(\Omega)}\frac{\|u^s-\widetilde{u}_h^s\|_0}{\|f\|_0}\lesssim h^{\min(t+1,2)}.$$

□

Remark 6.2. We observe that if $f\in\mathcal{E}_\mu$ then, thanks to the L^2-*a priori* error estimate in Remark (4.3), it holds

$$\|(T-\widetilde{T}_h)_{|E_\mu}\|_{\mathcal{L}(L^2(\Omega))}=\sup_{f\in\mathcal{E}_\mu}\frac{\|Tf-\widetilde{T}_hf\|_0}{\|f\|_0}=\sup_{f\in\mathcal{E}_\mu}\frac{\|u^s-\widetilde{u}_h^s\|_0}{\|f\|_0}\leq Ch^{t+1}.$$

Putting together Theorem 5.1 ,Theorem 6.1, and Remark 6.2, we can state the following result.

Theorem 6.3. *Let μ be an eigenvalue of T, with multiplicity m, and denote the corresponding eigenspace by E_μ. Then, exactly m discrete eigenvalues $\widetilde{\mu}_{1,h},\dots,\widetilde{\mu}_{m,h}$ (repeated according to their respective multiplicities) converge to μ. Moreover, let $\widetilde{E}_{\mu,h}$ be the direct sum of the eigenspaces corresponding to the discrete eigenvalues $\widetilde{\mu}_{1,h},\cdots,\widetilde{\mu}_{m,h}$ converging to μ. Then*

$$\delta(E_\mu,\widetilde{E}_{\mu,h})\leq Ch^{t+1}. \tag{6.2}$$

A direct consequence of the previous result (*cf.* [8,20]) is the following one.

Theorem 6.4. *Let u be a unit eigenfunction associated with the eigenvalue λ of multiplicity m and let $\widetilde{w}_h^{(1)},\dots,\widetilde{w}_h^{(m)}$ denote linearly independent eigenfunctions associated with the m discrete eigenvalues converging to λ. Then there exists $\widetilde{u}_h\in span\{\widetilde{w}_h^{(1)},\dots,\widetilde{w}_h^{(m)}\}$ such that*

$$\|u-\widetilde{u}_h\|_0\leq Ch^{t+1},$$

where $t=\min\{k,r\}$, being k the order of the method and r the regularity index of u.

Using Theorem 4.2 we can obtain an estimate of the conformity error (3.6) better than the one in Lemma 3.2 when its arguments are the solution to the continuous problem (2.5) and the discrete problem (4.15). It is worth noting that the solution to the discrete problem does not need to be an approximation of the solution to the continuous problem, *cf.* [20].

Lemma 6.5. *Consider $u \in H^{1+r}(\Omega)$, $v \in L^2(\Omega)$ and let $Tu, Tv \in H^{1+r}(\Omega)$ with $r > 1/2$ be, respectively, the solutions to problem (2.5) with load term u and v. Assume that* **(A0)** *is satisfied and let $\widetilde{T}_h u \in V_k^h \subset H^{1,nc}(\Omega_h; k)$ for some integer $k \geq 1$ be the virtual element approximation of Tu that solves problem (4.15). Then, there exists a constant $C > 0$, independent of h, such that*

$$|\mathcal{N}_h(Tv, \widetilde{T}_h u)| \leq C h^{2t} \, |Tv|_{1+r} \, |Tu|_{1+r} \tag{6.3}$$

where $t = \min\{k, r\}$ and $\mathcal{N}_h(u, v)$ is the conformity error defined in (3.6).

Proof. We start the following chain of developments from the definition of the conformity error given in (3.6), note that $[\![Tu]\!] = 0$ on every mesh side and that the moments up to order $k-1$ of $[\![\widetilde{T}_h u]\!]$ across all mesh interfaces are zero, and apply the Cauchy-Schwarz inequality in the last two steps:

$$\begin{aligned}
\mathcal{N}_h(Tv, \widetilde{T}_h u) &= \sum_{\sigma \in \mathcal{S}_h} \int_\sigma \nabla Tv \cdot [\![\widetilde{T}_h u]\!] \, \mathrm{d}\sigma \\
&= \sum_{\sigma \in \mathcal{S}_h} \int_\sigma (I - \Pi_{k-1}^{0,\sigma}) \nabla Tv \cdot (I - \Pi_0^{0,\sigma}) [\![\widetilde{T}_h u]\!] \, \mathrm{d}\sigma \\
&= \sum_{\sigma \in \mathcal{S}_h} \int_\sigma (I - \Pi_{k-1}^{0,\sigma}) \nabla Tv \cdot \Big((I - \Pi_0^{0,\sigma}) [\![\widetilde{T}_h u]\!]) - (I - \Pi_0^{0,\sigma}) [\![Tu]\!] \Big) \, \mathrm{d}\sigma \\
&= \sum_{\sigma \in \mathcal{S}_h} \int_\sigma (I - \Pi_{k-1}^{0,\sigma}) \nabla Tv \cdot (I - \Pi_0^{0,\sigma}) [\![(\widetilde{T}_h - T) u]\!] \, \mathrm{d}\sigma \\
&\leq \sum_{\sigma \in \mathcal{S}_h} \| (I - \Pi_{k-1}^{0,\sigma}) \nabla Tv \cdot \mathbf{n}_\sigma \|_{0,\sigma} \, \| (I - \Pi_0^{0,\sigma}) [\![(\widetilde{T}_h - T) u]\!] \cdot \mathbf{n}_\sigma \|_{0,\sigma} \\
&\leq \left[\sum_{\sigma \in \mathcal{S}_h} \| (I - \Pi_{k-1}^{0,\sigma}) \nabla Tv \cdot \mathbf{n}_\sigma \|_{0,\sigma}^2 \right]^{\frac{1}{2}} \times \left[\sum_{\sigma \in \mathcal{S}_h} \| (I - \Pi_0^{0,\sigma}) [\![(\widetilde{T}_h - T) u]\!] \cdot \mathbf{n}_\sigma \|_{0,\sigma}^2 \right]^{\frac{1}{2}} \\
&= \mathcal{N}_1 \times \mathcal{N}_2.
\end{aligned}$$

Trace inequality (3.18) yields

$$\| (I - \Pi_{k-1}^{0,\sigma}) \nabla Tv \cdot \mathbf{n}_\sigma \|_{0,\sigma} \lesssim h_\sigma^{t-\frac{1}{2}} |Tv|_{1+r,\Omega_\sigma},$$

and summing over all the mesh sides, noting that $h_\sigma \leq h$, the number of sides per element is uniformly bounded due to **(A0)** and using definition (3.3) yield

$$|\mathcal{N}_1|^2 = \sum_{\sigma \in \mathcal{S}_h} \| (I - \Pi_{k-1}^{0,\sigma}) \nabla Tv \cdot \mathbf{n}_\sigma \|_{0,\sigma}^2 \lesssim \left(h^{t-\frac{1}{2}} \right)^2 \sum_{\sigma \in \mathcal{S}_h} |Tv|_{1+r,\Omega_\sigma}^2 \lesssim \left(h^{t-\frac{1}{2}} \right)^2 \sum_{P \in \Omega_h} |Tv|_{1+r,P}^2,$$

and finally

$$|\mathcal{N}_1| \lesssim h^{t-\frac{1}{2}} |Tv|_{1+r}.$$

Similarly, trace inequality (3.18) and the jump definition yield

$$\| (I - \Pi_0^{0,\sigma}) [\![(\widetilde{T}_h - T) u]\!] \cdot \mathbf{n}_\sigma \|_{0,\sigma} \lesssim h_\sigma^{\frac{1}{2}} |(\widetilde{T}_h - T) u|_{1,\Omega_\sigma}$$

and using the same arguments as above we have that

$$\begin{aligned}
|\mathcal{N}_2|^2 &= \sum_{\sigma \in \mathcal{S}_h} \| (I - \Pi_0^{0,\sigma}) [\![(\widetilde{T}_h - T) u]\!] \cdot \mathbf{n}_\sigma \|_{0,\sigma}^2 \lesssim h \sum_{\sigma \in \mathcal{S}_h} |(\widetilde{T}_h - T) u|_{1,\Omega_\sigma}^2 \lesssim h \sum_{P \in \Omega_h} |(\widetilde{T}_h - T) u|_{1,P}^2 \\
&\lesssim h |(\widetilde{T}_h - T) u|_{1,h}^2.
\end{aligned}$$

Using this relation and the *a priori* error estimate in the energy norm of Remark 4.3 finally yield:

$$|\mathcal{N}_2| \lesssim h^{t+\frac{1}{2}}|Tu|_{1+r}.$$

The assertion of the lemma follows by collecting the above estimates together. □

We now prove the usual double order convergence of the eigenvalues.

Theorem 6.6. *Let λ be an eigenvalue of problem (2.2) with multiplicity m, and denote by $\widetilde{\lambda}_{1,h},\cdots,\widetilde{\lambda}_{m,h}$ the m discrete eigenvalues converging towards λ. Then the following optimal double order convergence holds:*

$$|\lambda - \widetilde{\lambda}_{i,h}| \leq Ch^{2t} \quad \forall i = 1,\dots,m, \tag{6.4}$$

with $t = \min\{k, r\}$, being k the order of the method and r the regularity index of the eigenfunction corresponding to λ.

Proof. We use the result stated in Theorem 5.2. It is clear that the second term in the estimate of Theorem 5.2 is of double order compared to the H^1-rate of convergence. Hence, we analyse in detail the term $b\left((T-\widetilde{T}_h)\phi_j,\phi_k\right)$. Let u and v be two eigenfunctions associated with the eigenvalue λ. Then, we note that $(T-\widetilde{T}_h)u \in H^{1,nc}(\Omega_h;k)$ and begin the chain of developments that follows from the definition of the conformity error in (3.6):

$$\begin{aligned}
b\left((T-\widetilde{T}_h)u,v\right) &= a(Tv,(T-\widetilde{T}_h)u) - \mathcal{N}_h(Tv,(T-\widetilde{T}_h)u) && \left[\text{note that } \mathcal{N}_h(Tv,Tu)=0\right]\\
&= a(Tv,(T-\widetilde{T}_h)u) + \mathcal{N}_h(Tv,\widetilde{T}_h u) && \left[\text{add and subtract } \widetilde{T}_h v \text{ in the first term}\right]\\
&= a((T-\widetilde{T}_h)v,(T-\widetilde{T}_h)u) + a(\widetilde{T}_h v,(T-\widetilde{T}_h)u) + \mathcal{N}_h(Tv,\widetilde{T}_h u) && \left[\text{split the middle term and use (3.6)}\right]\\
&= a((T-\widetilde{T}_h)v,(T-\widetilde{T}_h)u) + b(\widetilde{T}_h v,u) + \mathcal{N}_h(Tu,\widetilde{T}_h v)\\
&\quad - a(\widetilde{T}_h v,\widetilde{T}_h u) + \mathcal{N}_h(Tv,\widetilde{T}_h u) && \left[\text{add both sides of (4.15) }\right]\\
&= a((T-\widetilde{T}_h)v,(T-\widetilde{T}_h)u) + \left[b(u,\widetilde{T}_h v) - \widetilde{b}_h(u,\widetilde{T}_h v)\right] +\\
&\quad \left[a_h(\widetilde{T}_h v,\widetilde{T}_h u) - a(\widetilde{T}_h v,\widetilde{T}_h u)\right] + \left[\mathcal{N}_h(Tu,\widetilde{T}_h v) + \mathcal{N}_h(Tv,\widetilde{T}_h u)\right]\\
&= \textstyle\sum_{i=1}^4 \mathcal{R}_i.
\end{aligned}$$

Term $\mathcal{R}_1$ is clearly of order h^{2t}, being u and v eigenfunctions (see Rem. (4.3)):

$$|\mathcal{R}_1| = |a((T-\widetilde{T}_h)v,(T-\widetilde{T}_h)u)| \leq |(T-\widetilde{T}_h)v|_{1,h}\,|(T-\widetilde{T}_h)u|_{1,h} \lesssim h^{2t}.$$

To bound term $\mathcal{R}_2$ using the same computations in (4.14) and triangular inequality, we get

$$\begin{aligned}
|\mathcal{R}_2| &\lesssim \sum_{P\in\Omega_h} \|(I-\Pi_k^{0,P})u\|_{0,P}\,\|(I-\Pi_k^{0,P})\widetilde{T}_h v\|_{0,P}\\
&\lesssim \sum_{P\in\Omega_h} \|(I-\Pi_k^{0,P})u\|_{0,P}\,\left(\|(I-\Pi_k^{0,P})(T-\widetilde{T}_h)v\|_{0,P} + \|(I-\Pi_k^{0,P})Tv\|_{0,P}\right).
\end{aligned} \tag{6.5}$$

Now, note that

$$\|u-\Pi_k^{0,P}u\|_{0,P} \lesssim h^{\min(k+1,r+1)}|u|_{r+1,P} \lesssim h^{t+1}|u|_{r+1,P}. \tag{6.6}$$

By the continuity of L^2-projection with respect the L^2-norm we get

$$\|(I-\Pi_k^{0,P})(T-\widetilde{T}_h)v\|_{0,P} \leq \|(T-\widetilde{T}_h)v\|_{0,P}. \tag{6.7}$$

Moreover polynomial approximation estimate (3.16) yields

$$\|(I-\Pi_k^{0,P})Tv\|_{0,P} \lesssim h^{t+1}|Tv|_{1+r,P}. \tag{6.8}$$

Hence collecting (6.6), (6.7), (6.8) in (6.5), and using the L^2-*a priori* error estimate in Remark (4.3) and the stability estimate (2.6), we obtain

$$|\mathcal{R}_2| \lesssim h^{2t+2}|u|_{r+1}\,|Tv|_{r+1} \lesssim h^{2t+2}\|u\|_0\,\|v\|_0 \lesssim h^{2t+2}.$$

To estimate term $\mathcal{R}_3$, we first consider the developments:

$$a^P(\widetilde{T}_h u,\widetilde{T}_h v)-a_h^P(\widetilde{T}_h u,\widetilde{T}_h v)=a^P(\widetilde{T}_h u-(Tu)_\pi,\widetilde{T}_h v-(Tv)_\pi)+a_h^P(\widetilde{T}_h u-(Tu)_\pi,(Tv)_\pi-\widetilde{T}_h v),$$

where we make use of the consistency condition (4.4) to introduce $(Tu)_\pi$ and $(Tv)_\pi$, the elemental polynomial approximations of Tu and Tv that exist in accordance with (3.16). The terms on the right-hand side of the previous equation are similar and we can estimate both as follows:

$$|a^P(\widetilde{T}_h u-(Tu)_\pi,\widetilde{T}_h v-(Tv)_\pi)| \le \Big(|(\widetilde{T}_h-T)u|_{1,P}+|Tu-(Tu)_\pi|_{1,P}\Big)\Big(|(\widetilde{T}_h-T)v|_{1,P}+|Tv-(Tv)_\pi|_{1,P}\Big),$$

and, using the *a priori* error estimate in the broken H^1-norm in Remark (4.3), the local approximation properties of the VEM space by polynomials (3.16), and the stability estimate (2.6), it holds

$$\begin{aligned}
|\mathcal{R}_3| &\le \sum_{P\in\Omega_h}\Big|a^P(\widetilde{T}_h u,\widetilde{T}_h v)-a_h^P(\widetilde{T}_h u,\widetilde{T}_h v)\Big| \\
&\lesssim \Big(|(\widetilde{T}_h-T)u|_{1,h}+|Tu-(Tu)_\pi|_{1,h}\Big)\Big(|(\widetilde{T}_h-T)v|_{1,h}+|Tv-(Tv)_\pi|_{1,h}\Big) \\
&\lesssim h^{2t}|Tu|_{1+r}|Tv|_{1+r} \lesssim h^{2t}.
\end{aligned}$$

Finally, for term $\mathcal{R}_4$ we apply the triangle inequality, Lemma 6.5, and the stability estimate (2.6) to obtain:

$$|\mathcal{R}_4| \le |\mathcal{N}_h(Tu,\widetilde{T}_h v)|+|\mathcal{N}_h(Tv,\widetilde{T}_h u)| \lesssim h^{2t}|Tv|_{1+r}|Tu|_{1+r} \lesssim h^{2t}.$$

The assertion of the theorem follows from the above estimates. □

The proof of the optimal error estimate for the eigenfunctions in the discrete energy norm follows along the same line as the one for the nonconforming finite element method. We briefly report it here for the sake of completeness.

Theorem 6.7. *With the same notation as in Theorem 6.4, we have*

$$|u-\widetilde{u}_h|_{1,h} \le Ch^t,$$

where $t=\min(k,r)$, k *being the order of the method and* r *the regularity index of* u.

Proof.

$$u-\widetilde{u}_h=\lambda Tu-\widetilde{\lambda}_h\widetilde{T}_h\widetilde{u}_h=(\lambda-\widetilde{\lambda}_h)Tu+\widetilde{\lambda}_h(T-\widetilde{T}_h)u+\widetilde{\lambda}_h\widetilde{T}_h(u-\widetilde{u}_h),$$

then

$$|u-\widetilde{u}_h|_{1,h} \le |\lambda-\lambda_h|\,|Tu|_{1,h}+\lambda_h|(T-\widetilde{T}_h)u|_{1,h}+\widetilde{\lambda}_h|\widetilde{T}_h(u-\widetilde{u}_h)|_{1,h}.$$

The first term at the right-hand side of the previous equation is of order h^{2t}, while the second one is of order h^t. Finally, for the last term, using (4.5), the continuity of the operator $\widetilde{T}_h$, and Theorem 6.4, we obtain

$$\begin{aligned}
|\widetilde{T}_h(u-\widetilde{u}_h)|_{1,h}^2 &\le \frac{1}{\alpha_*}a_h(\widetilde{T}_h(u-\widetilde{u}_h),\widetilde{T}_h(u-\widetilde{u}_h)) \\
&= \frac{1}{\alpha_*}\widetilde{b}_h(u-\widetilde{u}_h,\widetilde{T}_h(u-\widetilde{u}_h)) \lesssim \|u-\widetilde{u}_h\|_0^2 \lesssim h^{2t+2}.
\end{aligned}$$

□

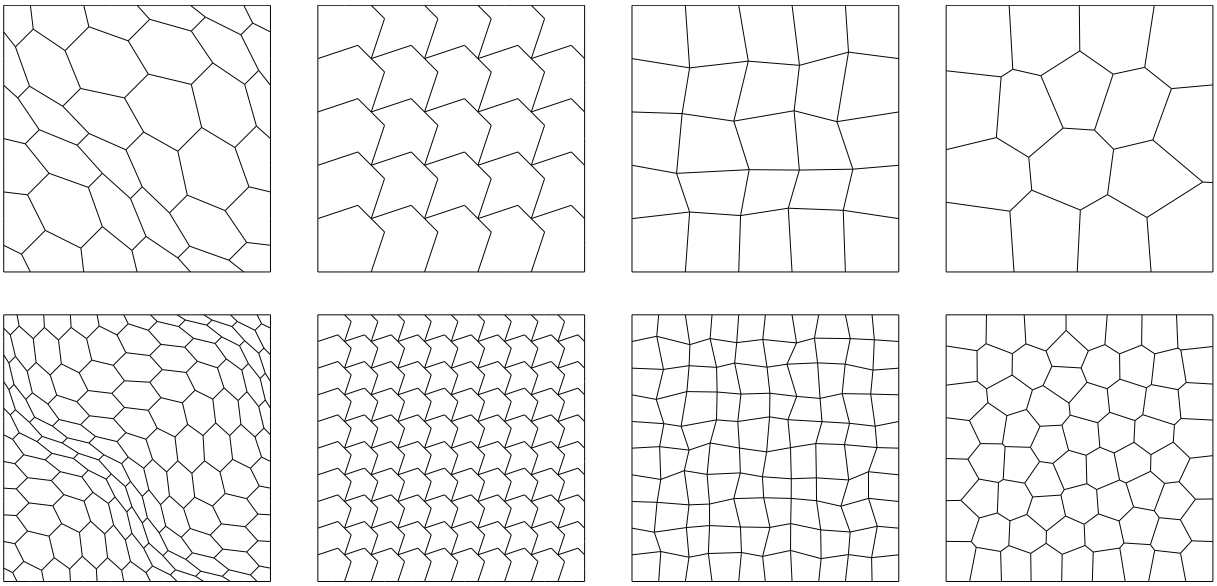

FIGURE 1. Base meshes (*top row*) and first refined meshes (*bottom row*) of the following mesh families from *left* to *right*: mainly hexagonal mesh; nonconvex octagonal mesh; randomized quadrilateral mesh; voronoi mesh.

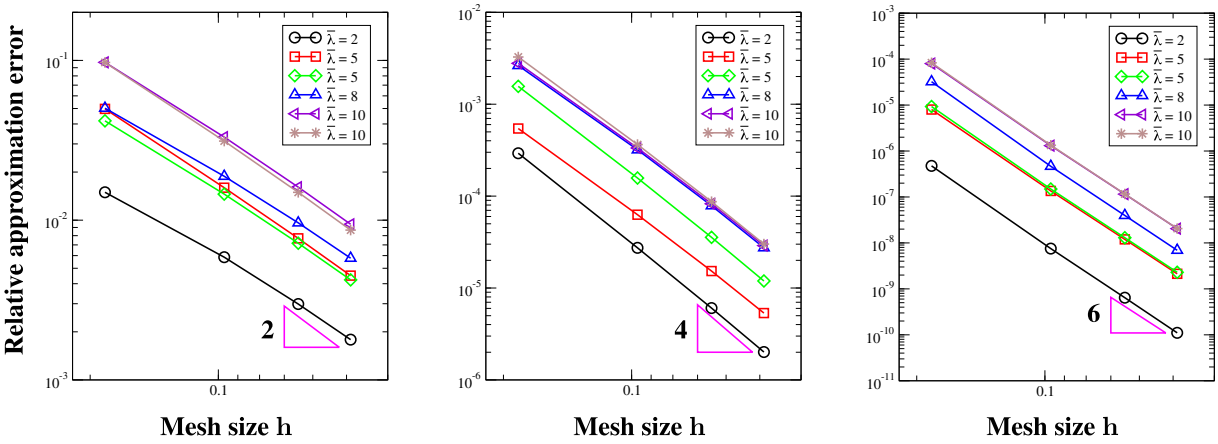

FIGURE 2. Test Case 1: Convergence plots for the approximation of the first six eigenvalues $\lambda = \pi^2\bar{\lambda}$ using the mainly hexagonal mesh and the nonconforming spaces: V_1^h (*left panel*); V_2^h (*mid panel*); V_3^h (*right panel*). The generalized eigenvalue problem uses the nonstabilized bilinear form $b_h(\cdot,\cdot)$.

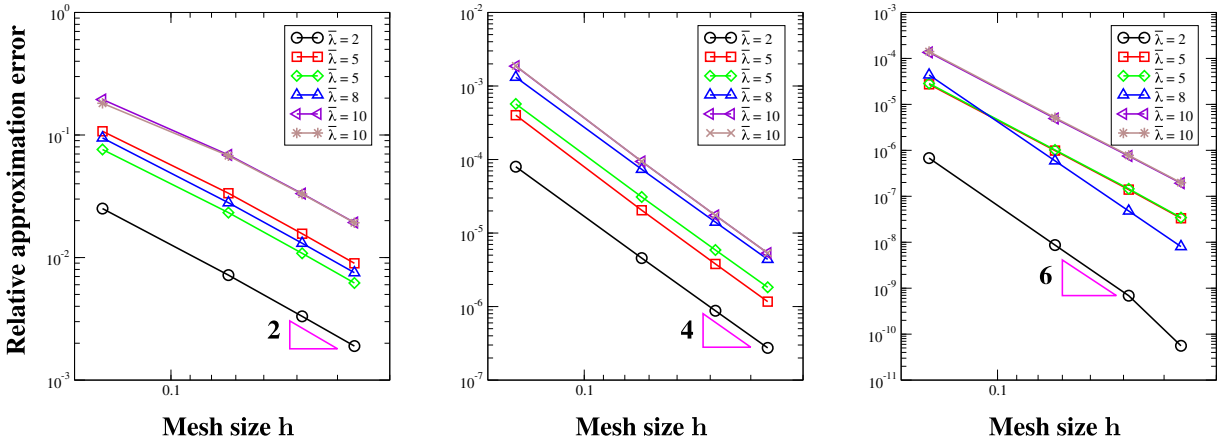

FIGURE 3. Test Case 1: Convergence plots for the approximation of the first six eigenvalues $\lambda = \pi^2\overline{\lambda}$ using the nonconvex octagon mesh and the nonconforming spaces: V_1^h (*left panel*); V_2^h (*mid panel*); V_3^h (*right panel*). The generalized eigenvalue problem uses the nonstabilized bilinear form $b_h(\cdot,\cdot)$.

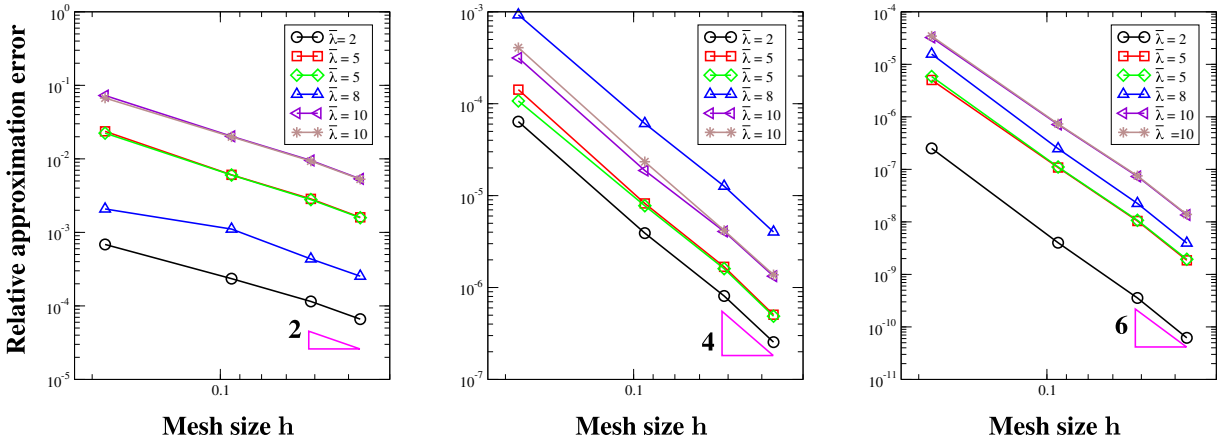

FIGURE 4. Test Case 1: Convergence plots for the approximation of the first six eigenvalues $\lambda = \pi^2\overline{\lambda}$ using the randomized quadrilateral mesh and the nonconforming spaces: V_1^h (*left panel*); V_2^h (*mid panel*); V_3^h (*right panel*). The generalized eigenvalue problem uses the nonstabilized bilinear form $b_h(\cdot,\cdot)$.

7. NUMERICAL EXPERIMENTS

In this section, we aim to confirm the optimal convergence rate of the numerical approximation of the eigenvalue problem (2.2) predicted by Theorems 6.6 for the nonconforming virtual element method. In particular, we present the performance of the nonconforming VEM applied to the eigenvalue problem on a two-dimensional square domain (Test Case 1) and on the L-shaped domain (Test Case 2). The convergence of the numerical eigenvalues is shown through the relative error quantity

$$\text{error}(\lambda) := \frac{|\lambda - \lambda_h|}{\lambda},$$

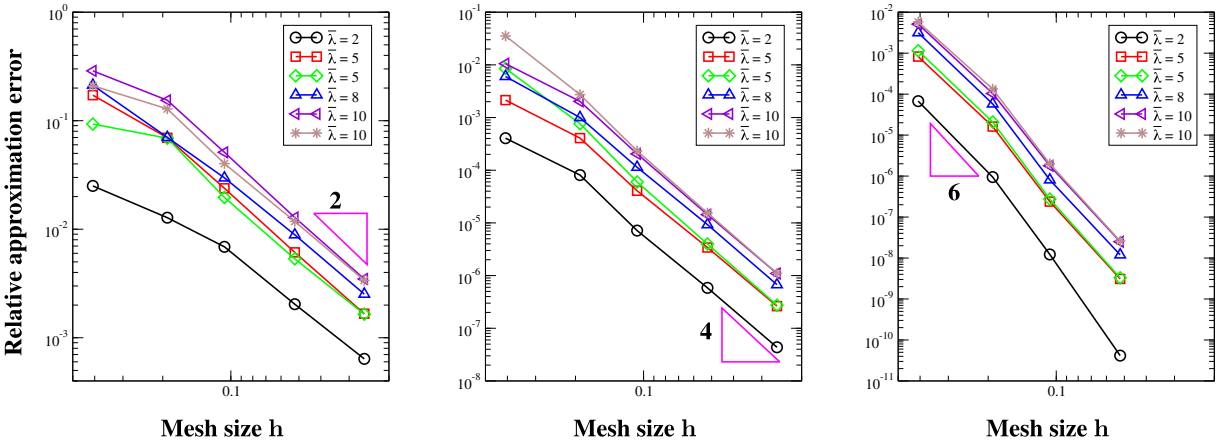

FIGURE 5. Test Case 1: Convergence plots for the approximation of the first six eigenvalues $\lambda = \pi^2\bar{\lambda}$ using the Voronoi mesh and the nonconforming spaces: V_1^h (*left panel*); V_2^h (mid panel); V_3^h (*right panel*). The generalized eigenvalue problem uses the nonstabilized bilinear form $b_h(\cdot,\cdot)$.

where λ denotes an eigenvalue of the continuous problem and λ_h its virtual element approximation. For Test Case 1, we also compare the error curves for the nonconforming and the conforming VEM of Reference [42]. For both test cases, we use the scalar stabilization for the bilinear form $a_h^P(\cdot,\cdot)$ and $\widetilde{b}_h^P(\cdot,\cdot)$, which reads as follows:

$$S^P(v_h, w_h) = \sigma_P \mathbf{v}_h^T \mathbf{w}_h,$$
$$\widetilde{S}^P(v_h, w_h) = \tau_P h^2 \mathbf{v}_h^T \mathbf{w}_h.$$

where $\mathbf{v}_h$, $\mathbf{w}_h$ denote the vectors containing the values of the local DoFs associated to v_h, $w_h \in V_k^h(P)$ and the stability parameters σ_P and τ_P are two positive constants independent of h. In the numerical tests, when $k = 1$, constant σ_P is the mean value of the eigenvalues of the matrix stemming from the consistency part of the local bilinear form a^P, *i.e.*, $a^P(\Pi_1^{\nabla,P}\cdot, \Pi_1^{\nabla,P}\cdot)$. For $k = 2, 3$, we set σ_P to the maximum eigenvalue of $a^P(\Pi_k^{\nabla,P}\cdot, \Pi_k^{\nabla,P}\cdot)$. Likewise, when $k = 1$, constant τ_P is set to the mean value of the eigenvalues of the matrix stemming from the consistency part of the local bilinear form $\frac{1}{h^2}b^P(\cdot,\cdot)$, *i.e.*, $\frac{1}{h^2}b^P(\Pi_1^{0,P}\cdot, \Pi_1^{0,P}\cdot)$. For $k = 2, 3$, we set τ_P to the maximum eigenvalue of $\frac{1}{h^2}b^P(\Pi_k^{0,P}\cdot, \Pi_k^{0,P}\cdot)$.

7.1. Test 1

In this test case, we numerically solve the standard eigenvalue problem with homogeneous Dirichlet boundary conditions on the square domain $\Omega =]0,1[\times]0,1[$. In this case, the eigenvalues of the problem are known and are given by:

$$\lambda = \pi^2(n^2 + m^2) \quad n, m \in \mathbb{N}, \text{ with } n, m \neq 0.$$

On this domain, we consider four different mesh partitionings, denoted by:

- *Mesh 1*, mainly hexagonal mesh with continuously distorted cells;
- *Mesh 2*, nonconvex octagonal mesh;
- *Mesh 3*, randomized quadrilateral mesh;
- *Mesh 4*, central Voronoi tessellation.

The base mesh and the first refined mesh of each mesh sequence is shown in Figure 1. These mesh sequences have been widely used in the mimetic finite difference and virtual element literature, and a detailed description

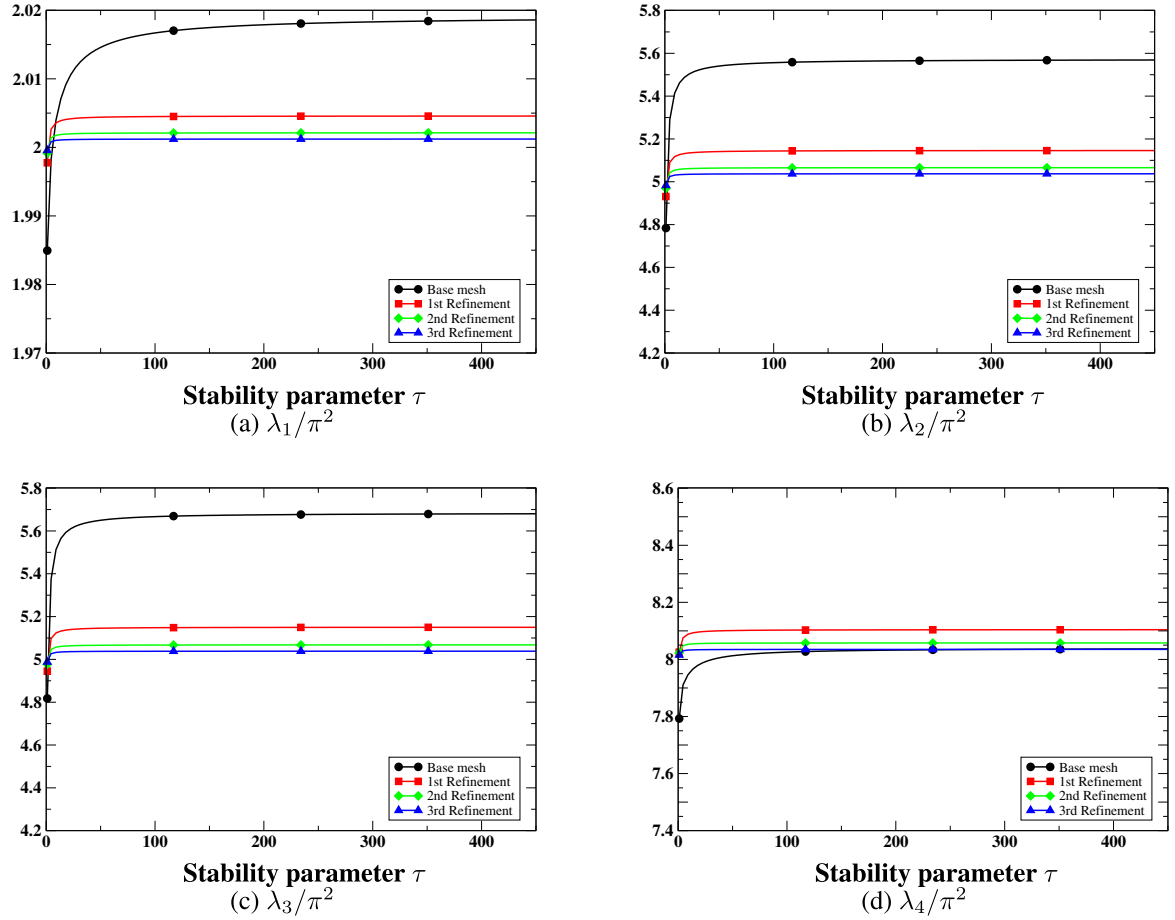

FIGURE 6. Test Case 1: Eigenvalue curves *versus* the stability parameter τ using the virtual element space V_1^h on the first four meshes of the mainly hexagonal mesh family.

of their construction can be found, for example, in [10]. We just mention that the last mesh sequence of central Voronoi tessellation is generated by the code PolyMesher [50].

The convergence curves for the four mesh sequences above are reported in Figures 2–5.

The expected rate of convergence is shown in each panel by the triangle close to the error curve and indicated by an explicit label. For these calculations, we used the VEM approximation based on the nonconforming space V_k^h, $k = 1, 2, 3$, and the VEM formulation (4.16) using the nonstabilized bilinear form $b_h(\cdot, \cdot)$. As already observed in [42] for the conforming VEM approximation, the same computations using formulation (4.17) and the stabilized bilinear form $\widetilde{b}_h(\cdot, \cdot)$ produce almost identical results, which, for this reason, are not shown here. These plots confirm that the nonconforming VEM formulations proposed in this work provide a numerical approximation with optimal convergence rate on a set of representative mesh sequences, including deformed and nonconvex cells.

In the four plots of Figure 6 we show the dependence on the stabilization parameter τ of the value of the first four eigenvalues $\lambda_1/\pi^2 = 2$, $\lambda_2/\pi^2 = 5$, $\lambda_3/\pi^2 = 5$, $\lambda_4/\pi^2 = 8$. From these plots, it is clear that the eigenvalue approximation is stable in a reasonable range of values of the parameter τ_P, and that the curves of the numerical eigenvalue converge to the corresponding eigenvalue.

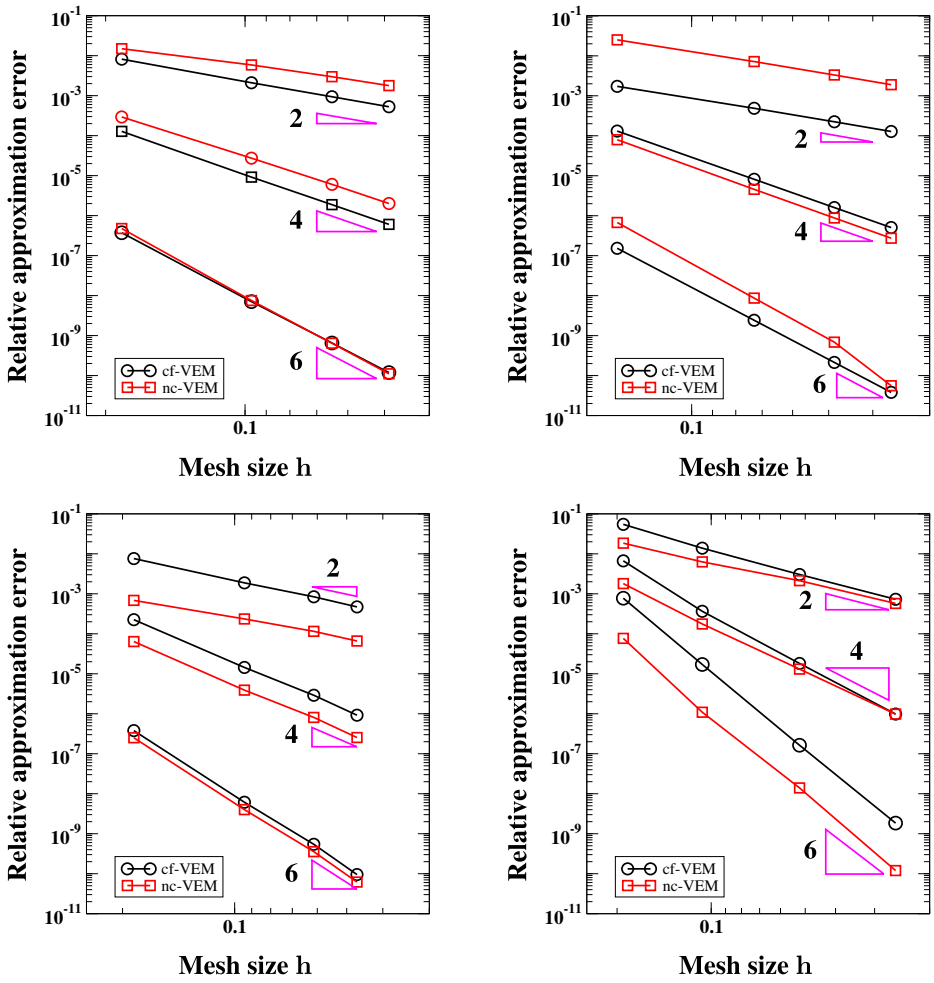

FIGURE 7. Test Case 1: Comparison *versus* h between the approximation of the first eigenvalue using the conforming and nonconforming VEM spaces V_k^h, $k = 1, 2, 3$, and the mainly hexagonal mesh (*top-left panel*); the nonconvex octagonal mesh (*top-right panel*); the randomized quadrilateral mesh (*bottom-left panel*); the Voronoi mesh (*bottom-right panel*).

In Figures 7 and 8 we compare the approximation of the first eigenvalue using the conforming and nonconforming VEM on the four mesh sequences *Mesh 1–Mesh 4*. The error curves are plotted *versus* the mesh size h in Figure 7 and the number of degrees of freedom in Figure 8.

For all these meshes, we see that the two approximations are very close.

7.2. Test 2

In this test case, we solve the eigenvalue problem with Neumann boundary conditions on the nonconvex L-shaped domain $\Omega = \Omega_1 \backslash \Omega_0$, where $\Omega_1 =]-1,1[\times]-1,1[$, and $\Omega_0 =]0,1[\times]-1,0[$. This test problem is taken from the benchmark suite of Reference [36]. For these calculations we use the Voronoi decompositions of Figure 9.

The convergence results relative to the first and third eigenvalue are shown in Figure 10. For the first eigenvalue, we observe a lower rate of convergence that is related to the fact the corresponding eigenfunction

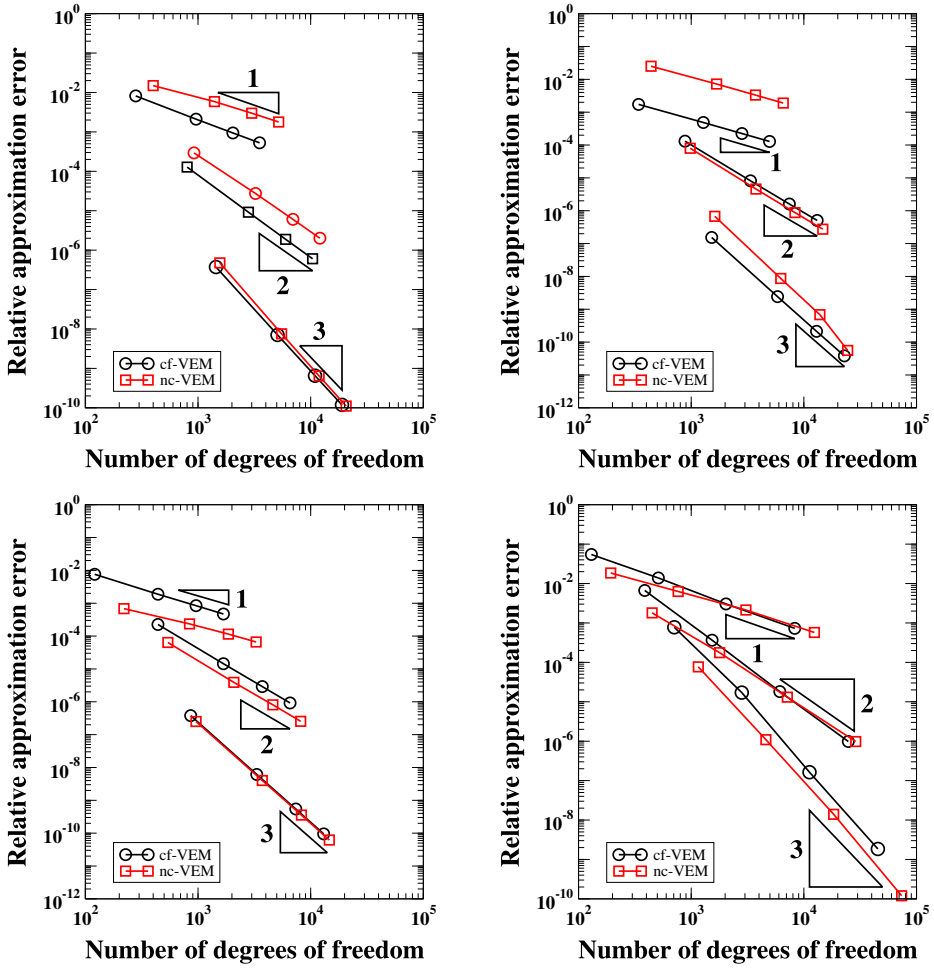

FIGURE 8. Test Case 1: Comparison *versus* the number of degree of freedom between the approximation of the first eigenvalue using the conforming and nonconforming VEM spaces V_k^h, $k = 1, 2, 3$, and the mainly hexagonal mesh (*top-left panel*); the nonconvex octagonal mesh (*top-right panel*); the randomized quadrilateral mesh (*bottom-left panel*); the Voronoi mesh (*bottom-right panel*).

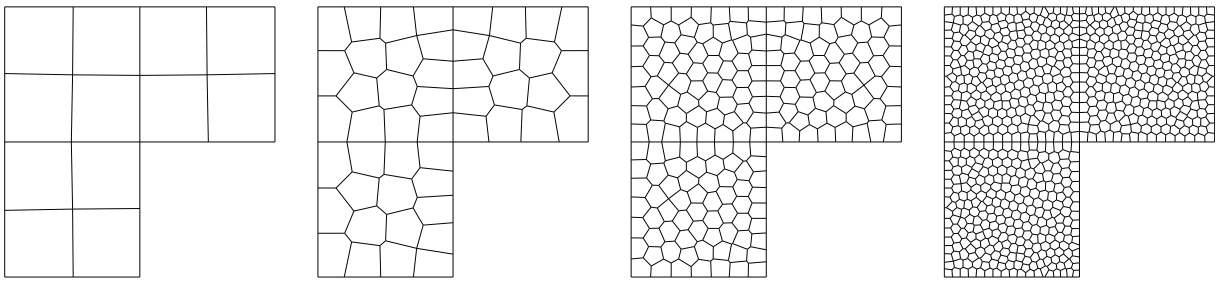

FIGURE 9. Test Case 2: Mesh sequence used in the L-shaped domain test.

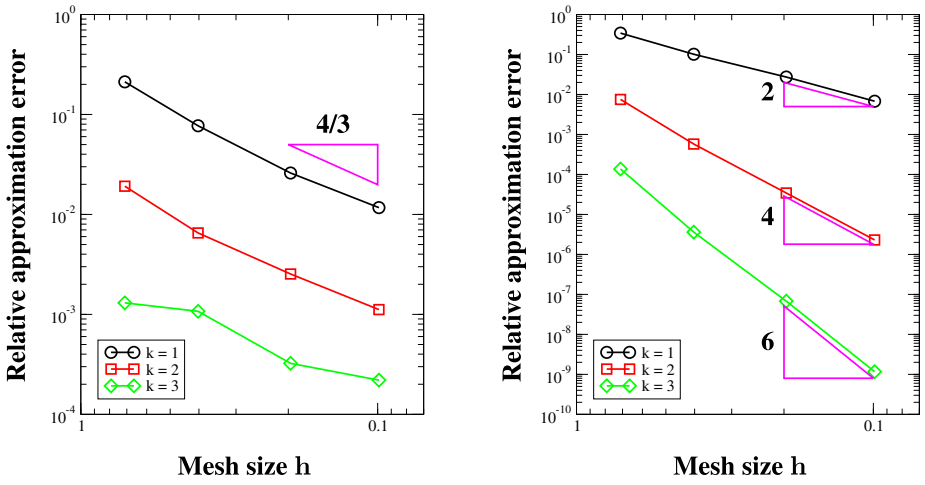

FIGURE 10. Test Case 2: convergence curves of the first eigenvalue (*left panel*) and the third eigenvalue (*right panel*) using the nonconforming VEM space V_k^h, $k = 1, 2, 3$.

belongs to $H^{1+r}(\Omega)$, with $r = 2/3 - \epsilon$ for any $\epsilon > 0$ (see [36]). Instead, the third eigenvalue is analytical and the optimal order of convergence is obtained, which can be seen by comparing the slopes of the error curves and the corresponding theoretical slopes reported on the plot. These results confirm the convergence analysis of the previous section and the optimality of the method also on nonconvex domains using polygonal meshes.

8. CONCLUSIONS

We analysed the nonconforming VEM for the approximation of elliptic eigenvalue problems. The nonconforming scheme, contrary to the conforming one, allows to use the same formulation both for the two- and the three-dimensional case. We proposed two different discrete formulations, which differ for the discrete form approximating the L^2-inner product. In particular, we considered both a nonstabilized form and a stabilized one. We showed that both formulations provide a correct approximation of the spectrum and we proved optimal *a priori* error estimates for the approximations of eigenfunctions both in the L^2-norm and the discrete energy norm, and the usual double order of convergence of the eigenvalues. Eventually, we presented a wide set of numerical tests which confirm the theoretical results.

Acknowledgements. The work of the second author was partially supported by the Laboratory Directed Research and Development Program (LDRD), U.S. Department of Energy Office of Science, Office of Fusion Energy Sciences, and the DOE Office of Science Advanced Scientific Computing Research (ASCR) Program in Applied Mathematics Research, under the auspices of the National Nuclear Security Administration of the U.S. Department of Energy by Los Alamos National Laboratory, operated by Los Alamos National Security LLC under contract DE-AC52-06NA25396.

REFERENCES

[1] R.A. Adams, Sobolev spaces. In Vol. 65 of *Pure and Applied Mathematics*. Academic Press, New York-London (1975).

[2] S. Agmon, Lectures on elliptic boundary value problems. In Vol. 2 of *Van Nostrand Mathematical Studies*. D. Van Nostrand Co., Inc., Princeton, NJ-Toronto-London (1965).

[3] B. Ahmad, A. Alsaedi, F. Brezzi, L.D. Marini and A. Russo, Equivalent projectors for virtual element methods. *Comput. Math. Appl.* **66** (2013) 376–391.

[4] P.F. Antonietti, L. Beirão da Veiga, S. Scacchi and M. Verani, A C^1 virtual element method for the Cahn–Hilliard equation with polygonal meshes. *SIAM J. Numer. Anal.* **54** (2016) 34–56.

[5] P.F. Antonietti, G. Manzini and M. Verani, The fully nonconforming virtual element method for biharmonic problems. *Math. Models Methods Appl. Sci.* **28** (2018) 387–407.
[6] E. Artioli, S. De Miranda, C. Lovadina and L. Patruno, A stress/displacement virtual element method for plane elasticity problems. *Comput. Meth. Appl. Mech. Eng.* **325** (2017) 155–174.
[7] B. Ayuso de Dios, K. Lipnikov and G. Manzini, The nonconforming virtual element method. *ESAIM: M2AN* **50** (2016) 879–904.
[8] I. Babuška and J. Osborn, Eigenvalue problems. In: Handbook of Numerical Analysis. *Handb. Numer. Anal. II*. North-Holland, Amsterdam (1991) 641–787.
[9] L. Beirão da Veiga, F. Brezzi, A. Cangiani, G. Manzini, L.D. Marini and A. Russo, Basic principles of virtual element methods. *Math. Models Methods Appl. Sci.* **23** (2013) 199–214.
[10] L. Beirão da Veiga, K. Lipnikov and G. Manzini, Arbitrary-order nodal mimetic discretizations of elliptic problems on polygonal meshes. *SIAM J. Numer. Anal.* **49** (2011) 1737–1760.
[11] L. Beirão da Veiga and G. Manzini, Residual *a posteriori* error estimation for the virtual element method for elliptic problems. *ESAIM: M2AN* **49** (2015) 577–599.
[12] L. Beirão da Veiga, D. Mora, G. Rivera and R. Rodríguez, A virtual element method for the acoustic vibration problem. *Numer. Math.* **136** (2017) 725–763.
[13] L. Beirão Da Veiga, F. Brezzi, F. Dassi, L.D. Marini and A. Russo, Serendipity virtual elements for general elliptic equations in three dimensions. *Chin. Ann. Math. Ser. B* **39** (2018) 315–334.
[14] L. Beirão da Veiga, F. Brezzi, L.D. Marini and A. Russo, Serendipity nodal vem spaces. *Comput. Fluids* **141** (2016) 2–12.
[15] L. Beirão Da Veiga, F. Dassi and A. Russo, High-order virtual element method on polyhedral meshes. *Comput. Math. Appl.* **74** (2017) 1110–1122.
[16] L. Beirão Da Veiga, C. Lovadina and A. Russo, Stability analysis for the virtual element method. *Math. Models Methods Appl. Sci.* **27** (2017) 2557–2594.
[17] L. Beirão da Veiga, C. Lovadina and G. Vacca, Divergence free virtual elements for the Stokes problem on polygonal meshes. *ESAIM: M2AN* **51** (2017) 509–535.
[18] L. Beirão da Veiga and G. Manzini, A virtual element method with arbitrary regularity. *IMA J. Numer. Anal.* **34** (2013) 759–781.
[19] M.F. Benedetto, S. Berrone, A. Borio, S. Pieraccini and S. Scialò, A hybrid mortar virtual element method for discrete fracture network simulations. *J. Comput. Phys.* **306** (2016) 148–166.
[20] D. Boffi, Finite element approximation of eigenvalue problems. *Acta Numer.* **19** (2010) 1–120.
[21] S.C. Brenner, Poincaré–Friedrichs inequalities for piecewise H^1 functions. *SIAM J. Numer. Anal.* **41** (2003) 306–324.
[22] S.C. Brenner, Q. Guan and L. Sung, Some estimates for virtual element methods. *Comput. Methods Appl. Math.* **17** (2017) 553–574.
[23] S.C. Brenner and L.R. Scott, The mathematical theory of finite element methods, 3rd edition. In Vol. 15 of *Texts in Applied Mathematics*. Springer, New York, NY (2008).
[24] F. Brezzi, A. Buffa and K. Lipnikov, Mimetic finite differences for elliptic problems. *ESAIM: M2AN* **43** (2009) 277–295.
[25] F. Brezzi and L.D. Marini, Virtual element methods for plate bending problems. *Comput. Methods Appl. Mech. Eng.* **253** (2013) 455–462.
[26] V. Calo, M. Cicuttin, Q. Deng and A. Ern, Spectral approximation of elliptic operators by the Hybrid High-Order Method. *J. Math. Comp.* **88** (2019) 1559–1586.
[27] A. Cangiani, F. Gardini and G. Manzini, Convergence of the mimetic finite difference method for eigenvalue problems in mixed form. *Comput. Methods Appl. Mech. Eng.* **200** (2011) 1150–1160.
[28] A. Cangiani, E.H. Georgoulis, T. Pryer and O.J. SUtton, A posteriori error estimates for the virtual element method. *Numer. Math.* **137** (2017) 857–893.
[29] A. Cangiani, V. Gyrya and G. Manzini, The nonconforming virtual element method for the Stokes equations. *SIAM J. Numer. Anal.* **54** (2016) 3411–3435.
[30] A. Cangiani, G. Manzini, A. Russo and N. Sukumar, Hourglass stabilization and the virtual element method. *Int. J. Numer. Meth. Eng.* **102** (2015) 404–436.
[31] A. Cangiani, G. Manzini and O.J. Sutton, Conforming and nonconforming virtual element methods for elliptic problems. *IMA J. Numer. Anal.* **37** (2017) 1317–1354.
[32] A. Chernov, L. Beirão da Veiga, L. Mascotto and A. Russo, Basic principles of *hp* virtual elements on quasiuniform meshes. *Math. Models Methods Appl. Sci.* **26** (2016) 1567–1598.
[33] H. Chi, L. Beirão da Veiga and G.H. Paulino, Some basic formulations of the virtual element method (VEM) for finite deformations. *Comput. Methods Appl. Mech. Eng.* **318** (2017) 148–192.
[34] P. Ciarlet, Basic error estimates for elliptic problems. In: Finite Element Methods (Part 1). In Vol. 2 of *Handbook of Numerical Analysis*. Elsevier (1991) 17–351.
[35] B. Cockburn, D.A. Di Pietro and A. Ern, Bridging the hybrid high-order and hybridizable discontinuous Galerkin methods. *ESAIM: M2AN* **50** (2016) 635–650.
[36] M. Dauge, Benchmark computations for Maxwell equations for the approximation of highly singular solutions. Available at: http://perso.univ-rennes1.fr/monique.dauge/benchmax.html (2004).
[37] D. Di Pietro, A. Ern and S. Lemaire, An arbitrary-order and compact-stencil discretization of diffusion on general meshes based on local reconstruction operators. *Comput. Methods Appl. Math.* **14** (2014) 461–472.

[38] D.A. Di Pietro, J. Droniou and G. Manzini, Discontinuous skeletal gradient discretisation methods on polytopal meshes. *J. Comput. Phys.* **355** (2018) 397–425.

[39] D.A. Di Pietro and A. Ern, Mathematical aspects of discontinuous Galerkin methods. In Vol. 69 of *Mathématiques & Applications (Berlin) [Mathematics & Applications]*. Springer, Heidelberg (2012).

[40] D.A. Di Pietro and A. Ern, Hybrid high-order methods for variable-diffusion problems on general meshes. *C. R. Math. Acad. Sci. Paris* **353** (2015) 31–34.

[41] A. Ern and J.-L. Guermond, Finite element quasi-interpolation and best approximation. *ESAIM: M2AN* **51** (2017) 1367–1385.

[42] F. Gardini and G. Vacca, Virtual element method for second order elliptic eigenvalue problems. *IMA J. Numer. Anal.* **38** (2018) 2026–2054.

[43] P. Grisvard, Singularities in boundary value problems and exact controllability of hyperbolic systems. In: Optimization, Optimal Control and Partial Differential Equations (Iaşi, 1992). In Vol. 107 of *Internat. Ser. Numer. Math.* Birkhäuser, Basel (1992) 77–84.

[44] T. Kato, Perturbation Theory for Linear Operators, 2nd edition. Springer-Verlag, Berlin (1976).

[45] K. Lipnikov and G. Manzini, High-order mimetic method for unstructured polyhedral meshes. *J. Comput. Phys.* **272** (2014) 360–385.

[46] L. Mascotto, I. Perugia and A. Pichler, Non-conforming harmonic virtual element method: h-and p-versions. *J. Sci. Comput.* **77** (2018) 1874–1908.

[47] D. Mora, G. Rivera and R. Rodríguez, A virtual element method for the Steklov eigenvalue problem. *Math. Models Methods Appl. Sci.* **25** (2015) 1421–1445.

[48] D. Mora, G. Rivera and R. Rodríguez. *A posteriori* error estimates for a virtual element method for the Steklov eigenvalue problem. *Comput. Math. Appl.* **74** (2017) 2172–2190.

[49] D. Mora, G. Rivera and I. Velásquez. A virtual element method for the vibration problem of kirchhoff plates. *ESAIM: M2AN* **52** (2018) 1437–1456.

[50] C. Talischi, G.H. Paulino, A. Pereira and I.F.M. Menezes, `PolyMesher`: a general-purpose mesh generator for polygonal elements written in Matlab. *Struct. Multidiscip. Optim.* **45** (2012) 309–328.

[51] G. Vacca, Virtual element methods for hyperbolic problems on polygonal meshes. *Comput. Math. Appl.* **74** (2017) 882–898.

[52] G. Vacca, An H^1-conforming virtual element for darcy and brinkman equations. *Math. Models Methods Appl. Sci.* **28** (2018) 159–194.

[53] P. Wriggers, W. Rust and B. Reddy, A virtual element method for contact. *Comput. Mech.* **58** (2016) 1039–1050.